

This is the preprint of the contribution published as:

Sühholz, S., Kopinke, F.-D., Mackenzie, K. (2022):

Heterogeneous activation of persulfate by FeS – Surface influence on selectivity

Chem. Eng. J. **450/3** , art. 138192

The publisher's version is available at:

<http://dx.doi.org/10.1016/j.cej.2022.138192>

Heterogeneous activation of persulfate by FeS – Surface influence on selectivity.

Sarah Sühnholz^{*a,b}, *Frank-Dieter Kopinke*^a and *Katrin Mackenzie*^a

^aHelmholtz Centre for Environmental Research - UFZ, Department of Environmental Engineering, Permoserstr. 15, D-04318 Leipzig, Germany

^bIntrapore GmbH, Katernberger Str. 107, D-45327 Essen, Germany

Corresponding Author

*Email: sarah.suehnholz@ufz.de. Phone: +493412351698

Abstract

Recently, several studies have been published on sulfate radicals as strong oxidants and methods of their generation. A shift from homogeneous to heterogeneous methods can be observed for persulfate activation as a means of generating sulfate radicals. However, to date, the influence of the surface on the radical chemistry has not been examined in detail.

In the present study, homogeneous persulfate activation methods (elevated temperature and dissolved iron(II)) are compared with heterogeneous activation by FeS. The selectivity patterns for the oxidation of chlorinated ethenes, ethanes and benzenes differ notably depending on the persulfate activation method. The obtained kinetic data are in conformity with the hypothesis that sulfate radicals generated at the FeS surface have different selectivities than freely dissolved radicals. The assumption of different reactive species is further confirmed by the determination of hydrogen kinetic isotope effects (H-KIEs) for the oxidation of methanol isotopologues with sulfate radicals using the set of activation methods. The H-KIE obtained in the heterogeneous system ($\text{H-KIE}_{\text{FeS}} = 3.0 \pm 0.3$) is significantly higher than for the

homogeneous system ($\text{H-KIE}_{\text{hom}} = 2.3 \pm 0.1$). This leads us to the conclusion that sulfate radicals generated on the FeS surface react as surface-associated radicals, which show a different selectivity pattern than freely dissolved radicals.

Furthermore, the apparent second-order rate constants in homogenous solution at ambient temperature, ranging from $4 \cdot 10^7$ to $1.7 \cdot 10^9 \text{ M}^{-1}\text{s}^{-1}$, were determined for the reaction of sulfate radicals with various chlorinated hydrocarbons under study.

KEYWORDS: persulfate activation; surface-associated sulfate radicals; iron sulfide; hydrogen kinetic isotope effects; second-order rate constants

1 Introduction

Increasing environmental awareness and still countless cases of polluted environmental compartments have led to a wide range of publications on chemical remediation methods in recent years [1-3]. Many of them are devoted to advanced oxidation processes (AOPs) in water, most of which use hydroxyl radicals ($\text{OH}\cdot$) as oxidants [4]. As a ‘newer oxidant’, research is increasingly focusing on sulfate radicals ($\text{SO}_4^{\cdot-}$) [5, 6]. Both radicals are among the strongest oxidizing agents, with standard reduction potentials for $\text{OH}\cdot/\text{H}_2\text{O}$ of about 2.73 V and for $\text{SO}_4^{\cdot-}/\text{SO}_4^{2-}$ of about 2.44 V [7]. While hydroxyl radicals react mostly via hydrogen abstraction or addition to double bonds, sulfate radicals are capable of one-electron transfer reactions in addition to hydrogen abstraction, which allows them to react with substances which are nonreactive towards hydroxyl radicals [8]. Sulfate radicals are highly electrophilic and allow fast reactions with electron-rich compounds, such as various benzenes, via the electron-transfer mechanism, which is however significantly slowed down by electron-withdrawing substituents such as chlorine, nitro or cyano substituents [9]. These substituent effects are much more pronounced than in the reaction with hydroxyl radicals, which leads to the statement that sulfate radicals react more selectively [8, 9]. Overall, there are a number of studies on the reactivity of

sulfate radicals with compounds of various structures and with different functional groups, which have also been supported with modeling attempts [10-16]. In general, for the hydrogen abstraction, the reaction rate constants decrease with the strength of the attacked C-H bonds and increase with the number of C-H bonds in the target molecule [11, 12, 15]. For the electron transfer from the substrate molecule to the sulfate radical, the availability of π -electrons in double bonds or aromatic groups is required [13, 15]. In this case, the reaction rate constants correlate mostly with the energy of the highest occupied molecular orbitals (E_{HOMO}) (or the difference between the energies of the lowest unoccupied molecular orbital (E_{LUMO}) and E_{HOMO}) and the charge density at the most probable electron transfer site in the compounds [14-16]. In comparison to electron transfer reactions, hydrogen abstraction by sulfate radicals is usually much slower. For most compounds, the rate constant of hydrogen abstraction is at least one order of magnitude lower for sulfate radicals compared to hydroxyl radicals [11, 17].

In order to generate the above-mentioned sulfate radical anions, peroxydisulfate (PS, $\text{S}_2\text{O}_8^{2-}$) activation can be used [5, 6]. This can be done either by energy input or single electron transfer to PS. By thermal activation or UV irradiation, PS is split into two free radicals (eq. 1), whereas the redox reaction only creates one radical per PS molecule (eq. 2) [18].



Since thermal or irradiation-induced activation of PS can be expensive or difficult to implement in some processes, activation via electron transfer has recently received increasing attention [19-23]. Redox-active iron species such as zero-valent iron (ZVI), dissolved Fe^{2+} and iron minerals have been most frequently studied for PS activation [5, 24-29]. The issue here, however, is that dissolved Fe^{2+} also reacts with sulfate radicals ($k = 9.9 \cdot 10^8 \text{ M}^{-1} \text{ s}^{-1}$ [30]) and

thus acts as competitor for the generated sulfate radicals, which may significantly lower the overall efficiency for pollutant degradation.

One way to overcome this challenge is to use a poorly water-soluble iron source like FeS [31-35]. Initially, FeS was reported to activate PS only as a slowly leaching Fe^{2+} source which initiates sulfate radical formation by homogenous reaction according to eq. (2) [31, 32]. However, since the reaction also takes place under basic and neutral pH conditions where FeS is almost insoluble, the assumption of a purely homogeneous activation mechanism needed to be discarded. In addition, it was found that the kinetics of FeS dissolution is slow since even after 100 h only 10% of the FeS was dissolved under strongly acidic reaction conditions [35, 36]. Recent findings furthermore indicate that the activation of PS on the surface of FeS takes place catalytically by surface-assisted homolytic bond cleavage [34, 35]. This was determined by measuring the radical yield, which was 1.6 mol $\text{SO}_4^{\cdot-}$ per mol $\text{S}_2\text{O}_8^{2-}$ indicating homolytic cleavage of the PS molecule [35]. A stoichiometric reaction of $\text{S}_2\text{O}_8^{2-}$ with Fe^{2+} could generate one mole per mole at most. These results also argue against the formation of Fe^{4+} , which was recently found as a reactive species in homogeneous PS activation with dissolved Fe^{2+} [5, 37, 38], since Fe^{4+} reacts mainly via a one-electron transfer to Fe^{3+} [39, 40] and thus would also give rise to a radical yield of at most one mole per mole. In contrast to PS, when peroxymonosulfate (PMS) was activated with FeS, Fe^{4+} species were found to be one of the reactive species [41], thus the activation of PMS was not investigated in this work. The present work is focussed exclusively on the activation of PS.

In addition, the highly recalcitrant water pollutant perfluorooctanoic acid (PFOA) was degraded by FeS-activated PS even when radical quenchers were present in the water matrix [36]. This led to the hypothesis that the sulfate radicals are formed directly on the FeS surface in close vicinity of the adsorbed PFOA. The actual reaction site at or near the surface is thus decoupled from any quenching reaction which would occur in solution [36]. Thus, FeS can activate PS

heterogeneously, and the surface plays a role in the selectivity of the radicals. Through sorption at the surface, locally higher pollutant concentrations can be achieved, which can lead to a change in substrate reactivity. Furthermore, sulfate radicals which are surface-associated could well have a different selectivity compared to freely dissolved sulfate radicals. Their lower mobility at the surface or a change in their electronic structure due to the surface influence could lead to the observed differences.

A powerful tool for characterizing selectivities of different radical species is to determine the hydrogen kinetic isotope effects (H-KIE = k_H/k_D), i.e. the ratio of rate constants for conversion of isotopologues of a substrate molecule [42]. Since a C-H bond is slightly weaker than a C-D bond (by about 5 kJ mol⁻¹), different reaction rate constants occur for H or D abstraction depending on the reactive species [43]. This difference is variable for various reactive species [44]. Hydroxyl radicals, for example, differentiate little between a C-H and a C-D bonds in the water phase [42]. Sulfate radicals, on the other hand, are more selective, so that H-abstraction proceeds significantly faster than D-abstraction [35]. Thus, based on the ratio of the reaction rate constants of H- and D-abstraction, differences in the type of reactive species can be identified [44]. In the present study, this method was applied in order to compare the selectivities of reactive species resulting from the homogeneous and FeS-catalyzed activation of PS. This influence has not yet been considered in the literature and is the subject of this work. Significantly different results from homogeneous and FeS activation would be another indication that activation with FeS is of heterogeneous nature.

The objective of this study is to provide a deeper understanding of the influence of the FeS surface on the selectivity of sulfate radicals. Therefore, we used three different kinds of model substances for the comparison of the selectivity patterns: (i) chlorinated ethenes and (ii) chlorinated benzenes, which both react via the electron-transfer mechanism, and (iii) chlorinated ethanes, which are attacked by hydrogen abstraction. These substances are easy to

analyze and are particularly suitable for selectivity analyses due to the large number of diverse substrate structures. In addition, the KIE of methanol oxidation with sulfate radicals was chosen in order to investigate whether the FeS surface affects the nature of the radical species, since CH₃OH and CD₃OH are expected to adsorb to FeS in a similar manner. Methanol is considered a well-suited probe molecule for KIE studies because the KIE can be determined from both (i) the reactant competition kinetics and (ii) the isotope composition of the primary oxidation product (formaldehyde). The oxidation products of the investigated chlorinated compounds were not part of this study and are described elsewhere [24, 45, 46].

2 Materials and Methods

2.1 Chemicals

1,2-Dichloroethane (1,2-DCA, 99.8%), 1,1,1,2-tetrachloroethane (1,1,1,2-TeCA, 99%), 1,1,2,2-tetrachloroethane (1,1,2,2-TeCA, 97%), *cis*-1,2-dichloroethene (*cis*-DCE, 97%), *trans*-1,2-dichloroethene (*trans*-DCE, 98%), 1,1-dichloroethene (1,1-DCE, 99%), trichloroethene (TCE, 99.5%), tetrachloroethene (PCE, 99%), 1,3-dichlorobenzene (1,3-DCB, 98%), 1,4-dichlorobenzene (1,4-DCB, 99%), 1,2,3-trichlorobenzene (1,2,3-TCB, 99%), 1,2,4-trichlorobenzene (1,2,4-TCB, 99%) and 1,2,3,4-tetrachlorobenzene (1,2,3,4-TeCB, 98%) were purchased from Sigma Aldrich. 1,1,2-Trichloroethane (1,1,2-TCA, 98%) was obtained from J & K Scientific, Belgium. 1,2,3,5-Tetrachlorobenzene (1,2,3,5-TeCB, 98%) was purchased from Riedel de Haën whereas vinyl chloride (VC, 99%) was purchased from Linde. Toluene-d₈ was obtained from Chemotrade. FeS (technical grade, $d_{50} = 20 \mu\text{m}$, $SSA_{\text{BET}} = 0.9 \text{ m}^2\text{g}^{-1}$) was received from Fluka. Na₂S₂O₈ (PS, >99%) was obtained from Roth whereas Na₂S₂O₃·5 H₂O (>99%) was obtained from J.T. Baker. Benzene (SupraSolv for GC), chloroform (GC grade), chlorobenzene (CB, p.a.), 1,2-dichlorobenzene (1,2-DCB, p.a.), H₂O₂ (35%), FeSO₄·7 H₂O (p.a.) and citric acid (CA, p.a.) were all purchased from Merck. Phenylhydrazine (>98%) was received from

Lancaster and methanol isotopologues were obtained either from CDN isotopes (CHD_2OH , 98.9%), DeuChem GmbH (CD_3OH , 99.8%) or Sulpelco (CH_3OH , hypergrade for LC-MS).

2.2 Selectivity experiments

Saturated chlorinated compounds and PS (200 mM) stock solutions were prepared with deionized water. The reactions were carried out in 60 mL crimped serum bottles without pH control. In the experiments with FeS and iron(II) citrate (FeCA), 0.3 g L^{-1} FeS or 5.4 mM FeCA, respectively and a defined amount of chlorinated compound stock solution were added to 50 mL of deionized water ($c_{0,\text{each chloroethene}} = 0.12 \text{ mM}$; $c_{0,\text{each chloroethane}} = 0.03 \text{ mM}$; $c_{0,\text{each chlorobenzene}} = 0.02 \text{ mM}$). In experiments studying chlorinated ethenes, the gas phase was sampled and analyzed using a GC-MS device (GC-MS-QP2010 Shimadzu, equipped with a HP5 capillary column, carrier gas was helium). For chlorinated ethanes and benzenes, 1 mL aqueous sample (maximum 10% of the total volume over the reaction duration) was taken and extracted with chloroform (spiked with either benzene as internal standard in case of chloroethanes as target or with toluene- d_8 when chlorobenzenes were studied). The addition of 1 mL of PS stock solution to the bottles marked the reaction start (t_0). For steady mixing of the suspension, the bottles were shaken at room temperature on a horizontal shaker at 250 rpm. The experiments with thermal activation were performed at $T = 30^\circ\text{C}$ and were similar to those described above for chlorinated ethanes and benzenes. For chlorinated ethenes, the glass vials were cooled down and equilibrated at room temperature before headspace sampling.

2.3 Kinetic isotope effects

100 mL of deionized water was spiked with 20 mM PS, 0.5 g L^{-1} FeS, and 12 mM each of CH_3OH and CD_3OH , then shaken continuously. After certain time periods (0.5 to 7 h), aliquots (0.5 mL) of the reaction suspension were withdrawn, filtered from FeS particles, quenched by adding a surplus of thiosulfate, and analyzed for methanol and formaldehyde by means of GC-

MS analysis. This allowed measurement of concentrations as well as isotope compositions. Methanol was analyzed by direct injection of aqueous samples, whereas formaldehyde was derivatized with phenylhydrazine, extracted and analyzed as phenylmethylenedrazone. The homogenous reaction was carried out similarly, but instead of FeS, UV light at 254 nm was used for the activation of PS or H₂O₂.

In most experiments the pH was not controlled. It decreased continuously from about 5 down to 1.5 due to the formation of sulfuric acid from PS decomposition. In an experiment with controlled pH, a stepwise addition of NaOH was performed such that the pH value remained in the range 3 to 2.

2.4 Calculation of apparent second-order reaction rate constants

Competition kinetics was used in order to compare the reactivities of solutes which were present together as a mix in the same solution, and thus react under identical reaction conditions. Therefore all chlorinated ethenes, ethanes or benzenes were mixed together in three separate batches. A detailed description of the calculation of apparent second-order rate constants $k_i^{\text{SO}_4^-}$ is given in the SI part in section 2. The formula used to calculate the apparent second-order rate constants is shown in eq. 3, where $c_{i,t}$ is the concentration of component i at time t .

$$\frac{\ln \frac{c_{A,t}}{c_{A,0}}}{\ln \frac{c_{B,t}}{c_{B,0}}} = \frac{k_A^{\text{SO}_4^-}}{k_B^{\text{SO}_4^-}} \quad (3)$$

2.5 Methodical approach

The influence of the activator surface on the reaction is a complex phenomenon. The surface can have an influence both on the generated radicals and on the reactive substrates. Especially with the substrates, adsorption plays a major role. In particular, the competitive adsorption should be mentioned here, which changes over the course of the reaction, since the most

adsorbing substances is expected to be enriched most at the surface, which in turn increases the probability of reaction with sulfate radicals formed in their neighborhood. At the same time, chloride is released into solution during the degradation of chlorinated compounds and can also react with the sulfate radicals. The chlorine radicals generated in this way are also able to react with the target compounds and presumably show a different selectivity pattern than the sulfate radicals. Due to the complexity of this situation, we have used various methods and evaluations. The comparison of relative rate constants obtained with different PS activation methods reflects different reaction selectivities, but does not reveal whether it is due to the ‘inherent’ selectivity of radical species or substrate adsorption. In order to resolve these two effects, we followed two approaches: (i) we considered the correlation between apparent reactivities and adsorption affinities of target compounds and (ii) we measured kinetic isotope effects. Following the first approach, we found higher apparent reactivities for less adsorbing substrates. Hence, the higher reactivity can be attributed to the selectivity of the radical species. The second approach is based on the assumption that isotopologues of the substrate behave very similar with respect to their adsorption but may react with significantly different rates because carbon-hydrogen bonds are broken. In addition to the *intermolecular* H-KIEs from competition experiments, we also determined *intramolecular* H-KIEs from product isotope analyses. This makes findings and mechanistic conclusions even more reliable.

As for the H-KIE, the double-logarithmic plot of the relative concentrations of two substances of a mixture can be used as tool for direct comparison of reaction systems. If the resulting slope of the regression line of the double-logarithmic plot remains constant over a broad range of conversion, it implies a consistent reaction mechanism, e.g. with a stationary radical pool. In our case it also rules out a shift of the radical pool from sulfate to chlorine radicals along the reaction progress (see also section SI 1).

3 Results and Discussion

3.1 Selectivity of sulfate radicals with various PS activation methods

For the investigation of selectivity patterns, oxidation of chloroorganic substances with homogeneous and heterogeneous PS activation were compared. The hypothesis is: if PS is activated heterogeneously, degradation of the target substances can also take place heterogeneously, i.e. in the adsorbed state. This would mean that the surface of the activator could have an influence on selectivity patterns of the degradation reaction. In addition, chlorinated ethanes are degraded by a different reaction mechanism with sulfate radicals than chlorinated ethenes and benzenes, i.e. hydrogen abstraction vs. electron transfer, respectively. These different reaction mechanisms could result in differently surface-affected selectivity patterns. Naturally, when the particulate activator FeS is used, proportions of homogeneous reaction may also occur in parallel; dissolved Fe^{2+} can react with PS and sulfate radicals formed at the FeS surface can desorb and diffuse into the aqueous bulk phase. We see a superposition of these effects.

3.1.1 Chlorinated ethenes

Figure 1 shows the double-logarithmic plot of the relative concentrations (c_0/c) of TCE and PCE in oxidation experiments with sulfate radicals (A) as well as the relative reaction rate constants of the chlorinated ethenes with sulfate radicals, normalized to that of PCE (B). The generation of the sulfate radicals was carried out with various methods of PS activation. Two different homogeneous activation methods were used to verify the results.

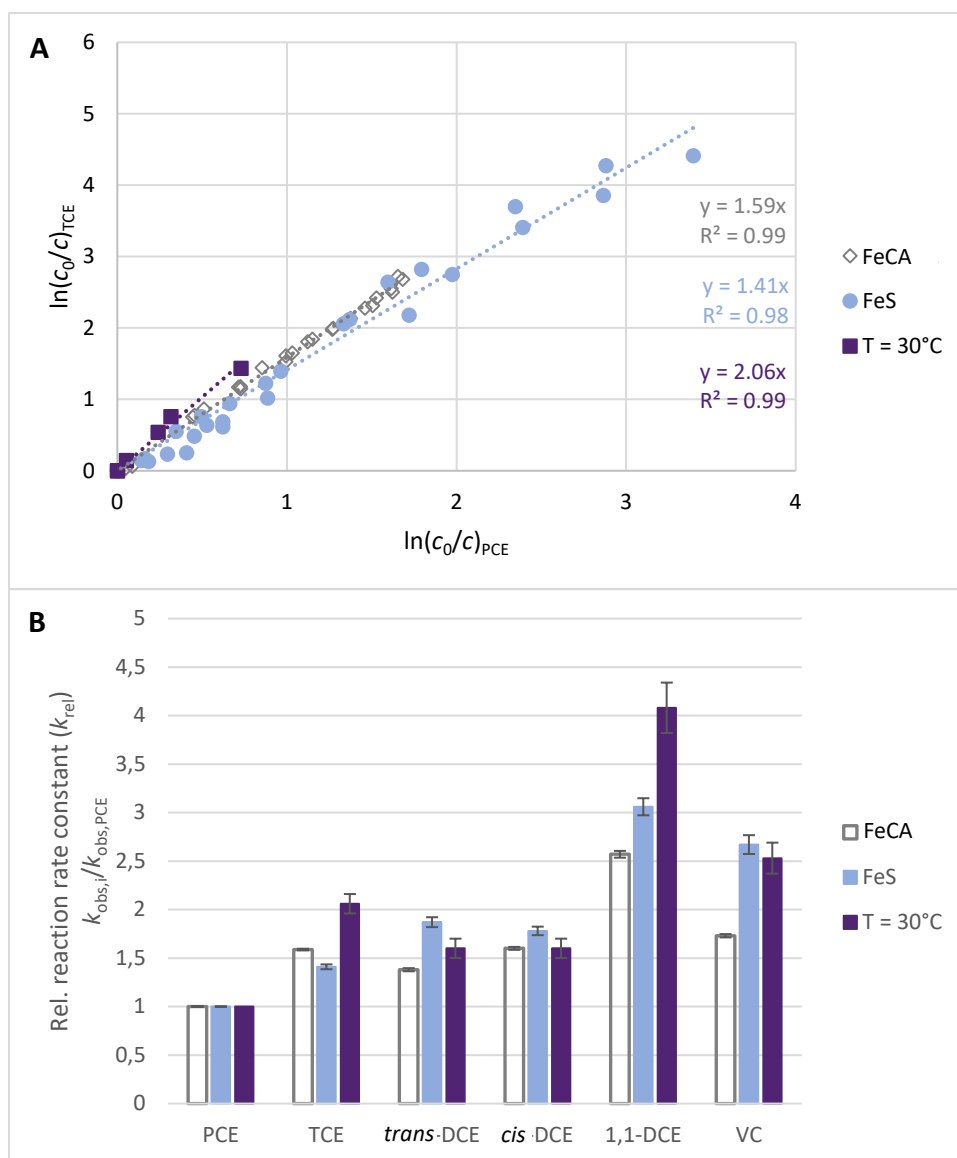


Figure 1: A) Example of the competition kinetics of TCE oxidation with sulfate radicals related to PCE oxidation. B) Relative reaction rate constants of chloroethenes oxidation with sulfate radicals. Sulfate radicals were generated by activation of PS with various activation methods ($c_{0,each\ chloroethene} = 120\ \mu\text{M}$; $c_{0,FeS} = 0.3\ \text{g L}^{-1}$; $c_{0,FeCA} = 5.4\ \text{mM}$; $c_{0,PS} = 4\ \text{mM}$; $\text{pH}_{start} = 7$; $\text{pH}_{final} = 2.4$). Error bars represent the standard deviations of the slopes of regression lines as shown in A).

The slopes of the regression lines shown in Figure 1A correspond to the relative reaction rate constant of TCE compared to PCE: $k_{rel,TCE} = k_{obs,TCE}/k_{obs,PCE}$. It can be seen that the regression lines for all three PS activation methods are strictly linear up to high TCE conversions. This indicates that there is no significant change in the pool of reactive species and no adsorption-related change in selectivity of the radicals during the reaction. Similar observations were made for the other chlorinated ethenes (Figures SI1B-3B). Figure 1B shows that there are only small

differences between relative rate constants obtained by PS activation with various methods. This is as to be expected when the oxidative species are identical. Furthermore, only small differences were observed between chlorinated ethenes depending on their degree and pattern of chlorination (< factor 3 in relative rate constants). This indicates that sulfate radicals practically do not distinguish between the substitution patterns in chlorinated ethenes. These results fit with data from the literature [13]. The similar substrate selectivity in thermally activated PS and FeS-assisted PS activation can possibly be explained by the fact that the chlorinated ethenes do not significantly adsorb to the FeS surface such that they are dominantly attacked by freely dissolved sulfate radicals. This indicates that freely dissolved sulfate radicals are the main reactive species in all three systems. When sulfate radicals are originally formed on the surface of the FeS, they are released into the water bulk phase and react as free radicals with the chlorinated ethenes. Therefore, the FeS surface does not play a major role in the oxidation reaction beyond the PS activation. In contrast, it is noticeable that the two homogeneous activation methods differ. In the literature it is described that Fe^{2+} can also react with PS to form Fe^{4+} as a reactive species [37, 47]. For this reason, PS experiments with methyl phenyl sulfoxide were carried out with FeCA as activator. This is an established method for quantification of Fe^{4+} species [37]. It was found that about 25% of the activated PS in our experimental setup yields Fe^{4+} (see Figure SI13). Even though this is only a quarter of the pool of reactive species, it may have an effect on the selectivity pattern. At the same time, it is another strong evidence that Fe^{4+} does not play a significant role in PS activation with FeS.

Table 1: Calculated apparent second-order rate constants k (in $10^9 \text{ M}^{-1} \text{ s}^{-1}$) at 20°C for reaction of chlorinated ethenes with sulfate radicals generated from PS with thermal activation at 30°C . k -values were calculated according to eq. 3 with PCE as reference.

Compound	k (in $10^9 \text{ M}^{-1} \text{ s}^{-1}$) at 20°C
PCE ¹⁾	0.67 ± 0.01
TCE	1.24 ± 0.05
<i>trans</i> -DCE	0.92 ± 0.08
<i>cis</i> -DCE	0.92 ± 0.11
1,1-DCE	2.35 ± 0.08
VC	1.44 ± 0.06

1) Value obtained from competition reaction with CB (see SI part).

3.1.2 Chlorinated ethanes

Figure 2A shows the double-logarithmic plot of 1,2-DCA oxidation versus 1,1,1,2-TeCA oxidation. As with the chloroethenes, the slope of the regression line is constant over the full range of conversion (see also Figures SI4B and 6B for the other chloroalkanes). Compared to chloroethenes, larger differences in the selectivity pattern between homogeneous and heterogeneous PS activation are obvious for chloroethanes (Figure 2B). Relative reaction rate constants vary up to a factor of 5. It should be mentioned that the homogeneous activation of persulfate using FeCA was not effective for the conversion of chloroethanes due to their low reactivity towards sulfate radicals and Fe^{4+} , respectively. These findings are in agreement with the literature [16].

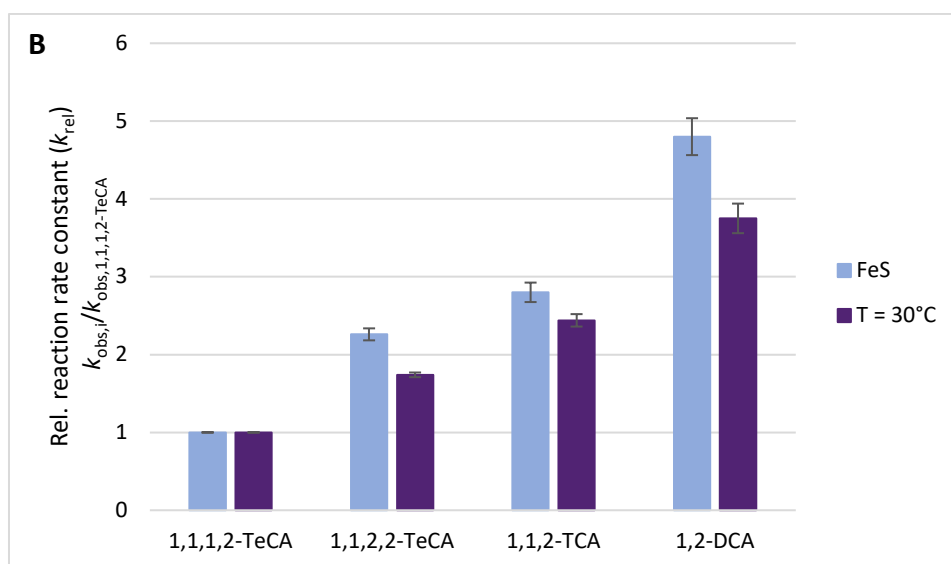
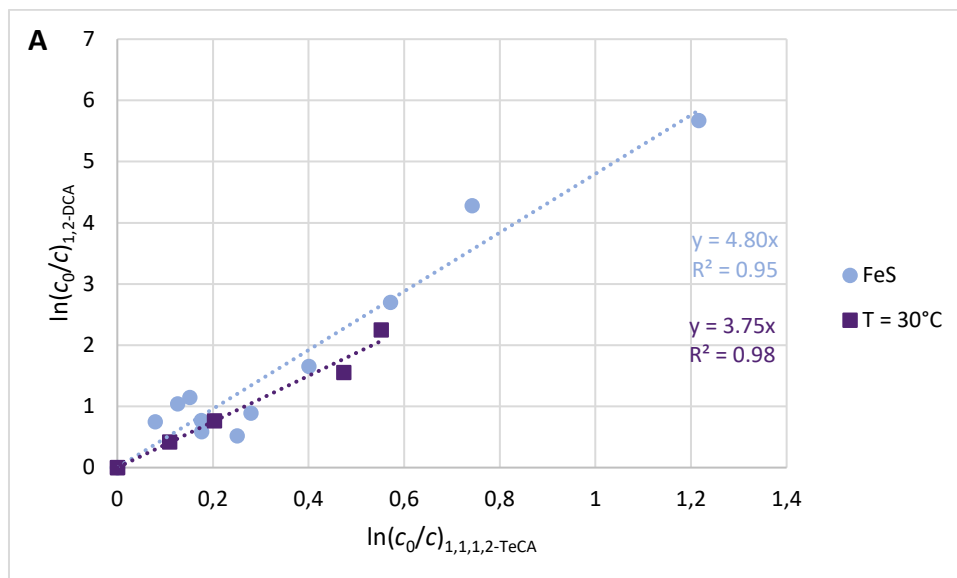


Figure 2: A) Example of the competition kinetics of 1,2-DCA oxidation with sulfate radicals related to 1,1,1,2-TeCA oxidation. B) Relative reaction rate constants of chloroethanes oxidation with sulfate radicals. Sulfate radicals were generated by activation of PS with various activation methods ($c_{0,\text{each chloroethane}} = 30 \mu\text{M}$; $c_{0,\text{FeS}} = 0.3 \text{ g L}^{-1}$; $c_{0,\text{PS}} = 4 \text{ mM}$; $\text{pH}_{\text{start}} = 7$; $\text{pH}_{\text{final}} = 2.4$). Error bars represent the standard deviations of the slopes of regression lines as shown in A).

The relatively low differentiation of sulfate radicals in their reaction with these chloroethanes in homogeneous solution, as shown in Figure 2B, is remarkable. This means that free sulfate radicals only slightly distinguish between the chlorine substitution patterns in the molecule (factors up to 4), although the reaction mechanism (H-abstraction) differs from that occurring with chloroethenes (one-electron transfer). When FeS is used as PS activator, the selectivity

pattern varies slightly. In this context, the possibility of reductive degradation of the compounds via FeS should be examined. For this purpose, experiments were carried out with hexachloroethane. After more than 5 hours of reaction time, no degradation of the hexachloroethane could be observed (see Figure SI5). Thus, one can exclude that reduction occurs at the FeS but also no reductive degradation by the persulfate radical, as recently shown for anaerobic conditions [48]. The reactivity of chloroethanes with sulfate radicals in aqueous solution is much lower than that of chloroethenes, which makes surface effects more significant. This is in conformity with the hypothesis that the selectivity-controlling step is surface-assisted, which indicates that surface-associated sulfate radicals and/or adsorbed substrates are involved.

Table 2: Calculated apparent second-order rate constants k (in $10^9 \text{ M}^{-1} \text{ s}^{-1}$) at 20°C for reaction of chlorinated ethanes with sulfate radicals generated from PS with thermal activation at 30°C . k -values were calculated according to eq. 3 with 1,2-DCA as reference.

Compound	k (in $10^9 \text{ M}^{-1} \text{ s}^{-1}$) at 20°C
1,1,1,2-TeCA	0.048 ± 0.001
1,1,2,2-TeCA	0.084 ± 0.003
1,1,2-TCA	0.117 ± 0.003
1,2-DCA ¹⁾	0.180 ± 0.004

1) Value obtained from competition reaction with CB (see SI part).

3.1.3 Chlorobenzenes

The third group of substances investigated in this study consists of eight chlorobenzenes. Also in this case, constant slopes of the linear regression lines in double-logarithmic coordinates were observed (see Figures 3A and SI7B, 10B, 11B). Chlorobenzenes also react with sulfate radicals via one-electron transfer, which results in high reaction rate constants. Despite the fast reaction with the radicals, we can still expect a significant influence of the FeS surface, since the substrates tend to adsorb on the FeS surface through the aromatic π -system, which should be affected by the substitution degree and pattern. The comparison of relative reaction rate constants is shown in Figure 3B.

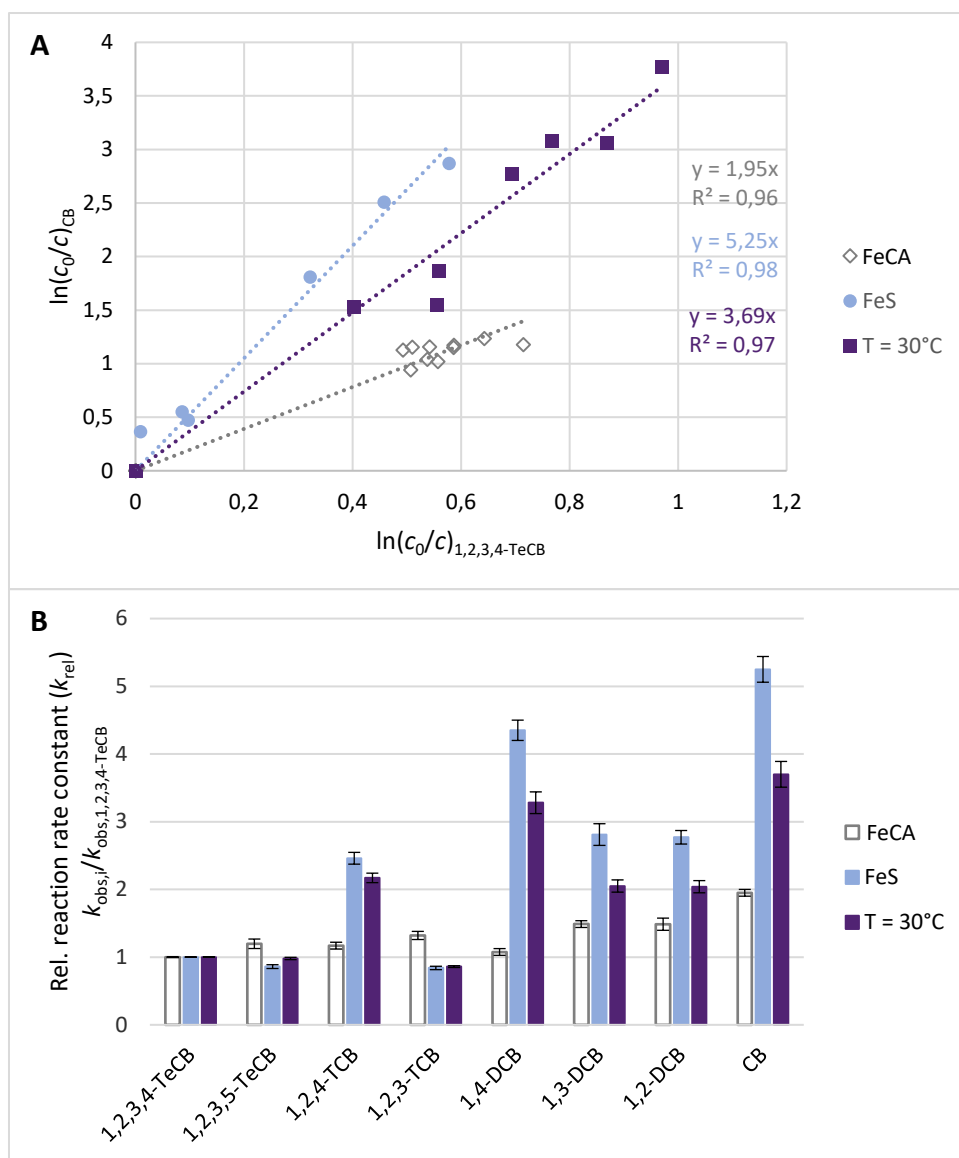


Figure 3: A) Example of the competition kinetics of CB oxidation with sulfate radicals related to 1,2,3,4-TeCB oxidation. **B)** Relative reaction rate constants of chlorobenzenes oxidation with sulfate radicals. Sulfate radicals were generated by activation of PS with various activation methods ($c_{0,each\ chlorobenzene} = 20\ \mu\text{M}$; $c_{0,FeS} = 0.3\ \text{g L}^{-1}$; $c_{0,FeCA} = 5.4\ \text{mM}$; $c_{0,PS} = 4\ \text{mM}$; $\text{pH}_{start} = 7$; $\text{pH}_{final} = 2.4$). Error bars represent the standard deviations of the slopes of regression lines as shown in A).

The first aspect that stands out here is that the relative reaction rate constants for the degradation of chlorobenzenes show only minor gradations when using FeCA as PS activator (up to a factor of 2 between CB and TeCBs). Thus, the influence of Fe^{4+} seems to be even more pronounced here in comparison to the degradation of chlorinated ethenes. This means that the observed selectivities with PS activation by FeCA cannot be used for the comparison between

homogeneous and heterogeneous activation with respect to sulfate radicals. Therefore, if mechanistic studies on persulfate activation/production of sulfate radicals are to be done, dissolved Fe^{2+} should not be utilized. When PS is activated heterogeneously using FeS particles, the gradation is more distinct (up to a factor of 5) and also differs from thermal activation. The lower the chlorine substitution degree is, the higher are the differences between homogeneous and heterogeneous PS activation. Although the reaction rate constants of sulfate radicals and chlorobenzenes are very high (similar to those of chloroethenes, compare Tables 1 and 3), adsorption of substrates may be expected to affect observable conversion rates. It is reasonable to assume that the adsorption affinity of chlorinated benzenes on FeS increases with rising number of chlorine atoms in the molecule. From Figure 3, we see that CB reacts 5 times faster than tetrachlorobenzenes in the FeS-activated system. This means that the difference in observable chlorobenzene selectivities is due to different *inherent* reactivities of the benzenes rather than to different adsorptive enrichment on the FeS surface. We consider this finding to be a indication for participation of surface-assisted oxidant species with a higher selectivity than freely dissolved sulfate radicals.

For the group of chlorobenzenes, some experiments with fixed pH value were also carried out in order to determine whether the differences between homogeneous and heterogeneous PS activation are due to pH changes during the reaction (see Figure SI9). However, the results show no significant differences. Thus, these data support our hypothesis that the observed selectivities are controlled by the mechanism of the PS activation.

Table 3: Calculated apparent second-order rate constants k (in $10^9 \text{ M}^{-1} \text{ s}^{-1}$) at 20°C for reaction of chlorinated benzenes with sulfate radicals generated from PS with thermal activation at 30°C . k -values were calculated according to eq. 3 with chlorobenzene as reference.

Compound	k (in $10^9 \text{ M}^{-1} \text{ s}^{-1}$) at 20°C
1,2,3,4-TeCB	0.41 ± 0.02
1,2,3,5-TeCB	0.40 ± 0.03
1,2,4-TCB	0.88 ± 0.08
1,2,3-TCB	0.35 ± 0.03
1,4-DCB	1.33 ± 0.14
1,3-DCB	0.83 ± 0.09
1,2-DCB	0.83 ± 0.09
CB ¹⁾	1.50

1) Value taken from [49].

Overall, the differences in the relative reaction rate constants of the individual substance groups are significant for heterogeneous PS activation. Less-chlorinated compounds mostly react faster than the higher-chlorinated ones. However, the most prominent point is that sulfate radicals from FeS-promoted PS activation show higher selectivities than sulfate radicals from homogeneous PS activation. In addition, FeS-activated PS can also lead to freely dissolved radicals, so that a large part of the pollutant reacts in the water phase instead of at the FeS surface. This makes the difference found for FeS and homogeneous PS activation even more evident. The combined findings suggest that a different reactive species is at work - probably surface-associated sulfate radicals. However, since the differences in selectivity are visible, but not significant enough to support the hypothesis, intra- and intermolecular hydrogen kinetic isotope effects (H-KIEs) were determined. They provide a powerful tool for distinguishing between different reactive species in homogeneous and heterogeneous chemical reactions.

3.2 Kinetic isotope effects

Although the evidence discussed in Section 3.1 points to selectivity differences of the radicals

originating from the various PS activation methods, the results therein only suggest that the FeS surface has a significant effect, but provide no information about the nature of this effect, *i.e.* whether it is due to different radical species or substrate adsorption. Therefore, the H-KIE was used to investigate whether the surface influences the radical species. H-KIEs provide a versatile tool for elucidating reaction mechanisms [42, 50]. Due to the different chemical reactivity of substrate isotopologues with reactive species, it is possible to distinguish between these species and different reaction pathways. In this study, methanol isotopologues (CH_3OH , CHD_2OH and CD_3OH) were used as target compounds in order to measure inter- and intramolecular KIEs. While in intermolecular KIE the competition between H- and D-abstraction by the attacking radicals takes place on different molecules, in intramolecular KIE the competition between H- and D-abstraction takes place in the same molecule. Figure 4 shows double-logarithmic plots of the relative concentrations (c_0/c) of methanol isotopologues from two oxidation experiments, with on the one hand hydroxyl radicals (from H_2O_2) and on the other hand sulfate radicals (from PS), in homogeneous solution. The slopes of the regression lines correspond to the intermolecular H-KIEs for hydrogen abstraction by hydroxyl and sulfate radicals. It can be seen that the regression lines are strictly linear up to high methanol conversion degrees ($\geq 99.8\%$). Furthermore, the estimated KIE for hydrogen abstraction from methanol by free sulfate radicals is about 2.3.

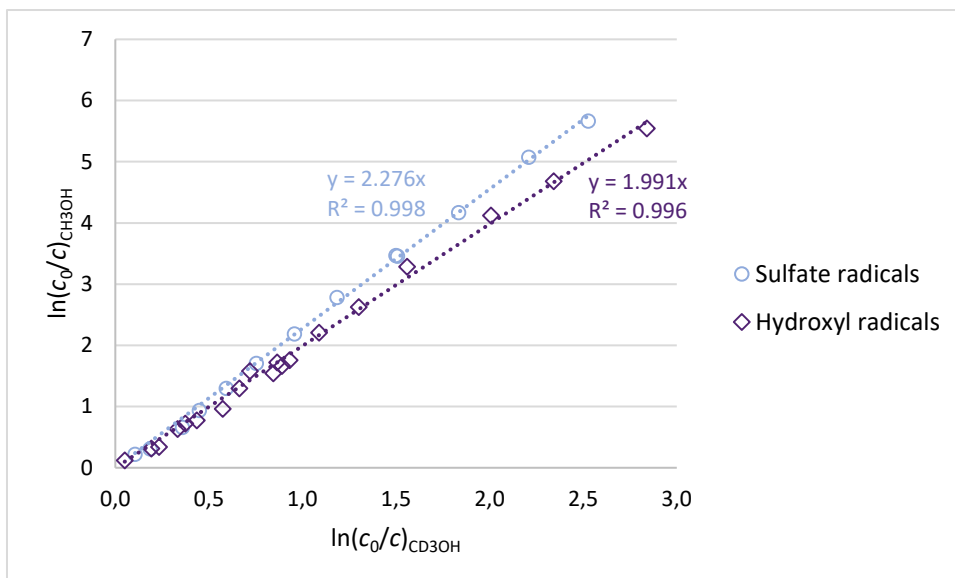


Figure 4: Oxidation of CH₃OH and CD₃OH (12 mM each) with H₂O₂ (45 mM) and PS (20 mM) in homogeneous solution, both UV (254 nm) activated.

Similar oxidation experiments with methanol as substrate and sulfate radicals as oxidant were carried out using FeS as PS activator in a heterogeneous reaction system. Figure 5 shows the same double-logarithmic plot of relative methanol concentrations as in Figure 4. In the case that the reactive species were to be the same in homogeneous and heterogeneous reactions, one would expect a straight line with the same slope as in Figure 4. However, in two independent experiments, one without and one with pH control, curved regression lines with different slopes were observed. This means that the curvature of the lines is not caused by pH changes during the reaction and shows therefore a shift in the primary H-KIEs of methanol oxidation. Interestingly, the final slopes (final H-KIEs) of 1.36 and 1.01 in the heterogeneous system are both below the characteristic H-KIEs of the sulfate (H-KIE = 2.28 ± 0.02) and hydroxyl radicals (H-KIE = 1.99 ± 0.02) in the homogenous system. Obviously, the oxidation of methanol by PS

follows different kinetics or even different reaction mechanisms in homogeneous solution to those in FeS suspension.

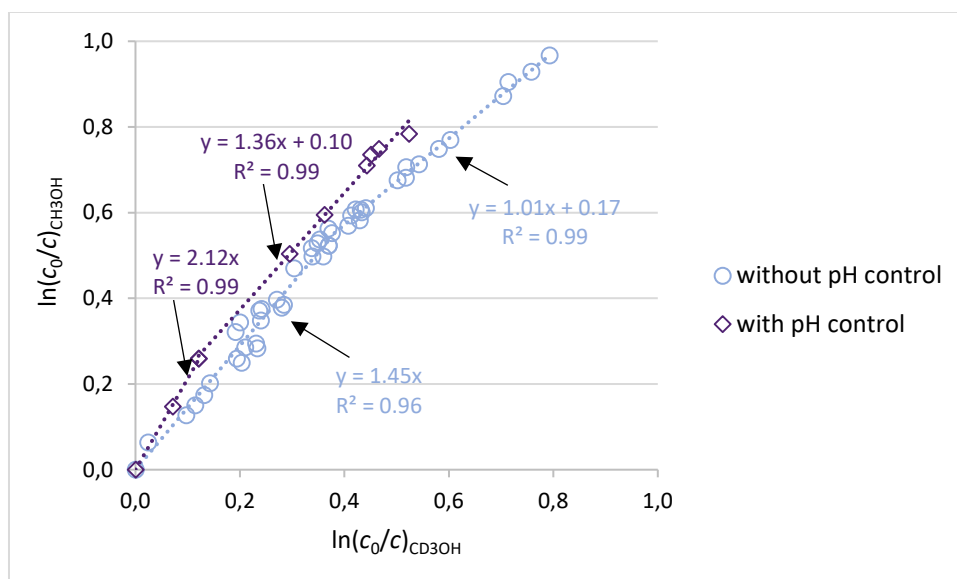
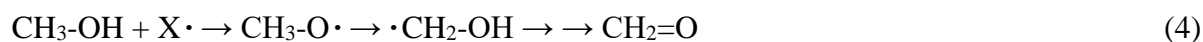


Figure 5: Oxidation of CH₃OH and CD₃OH (12 mM each) with PS (20 mM), activated by FeS (0.5 g L⁻¹) in suspension with (pH = 3-2) and without pH control (pH = 5-1.5).

The significantly smaller apparent intermolecular H-KIEs in the methanol conversion in the heterogeneous system compared to the homogeneous activation could be caused by an attack of the radicals on the hydroxyl group of the methanol. The hydroxyl group is the same in CH₃OH and CD₃OH and would therefore lead to H-KIEs around 1. Although this is not very likely, such a reaction pathway cannot be excluded. The subsequent intramolecular 1,2-hydrogen shift results in the same hydroxymethyl radical as in the abstraction of methyl hydrogen, which can also end in formaldehyde (see eq. 4).



Tracking the disappearance of reactants (as in Figures 4 and 5) yields reliable KIE values for high but hardly for low conversion degrees. In this case, isotopic analysis of the reaction products may be more suitable. The primary oxidation product of methanol is formaldehyde. Figure 6 shows the isotope composition of the formaldehyde formed along the reaction

progress. The formaldehyde becomes heavier (richer in D) the higher the methanol conversion is. This tendency may have three causes: (i) the enrichment of CD_3OH over CH_3OH , (ii) the subsequent formaldehyde oxidation with its own H-KIE and (iii) a shift in the primary H-KIEs of methanol oxidation, as indicated already by the curved lines in Figure 5. Hence, in order to obtain the primary H-KIE, the initial formaldehyde composition is needed. This composition can be obtained by extrapolating the data sets towards a methanol conversion of zero ($X \rightarrow 0$, $c/c_0 \rightarrow 1.0$) (eq. 5).

$$(c_{\text{CH}_2=\text{O}}/c_{\text{CD}_2=\text{O}})_{X \rightarrow 0} / (c_{\text{CH}_3\text{OH}}/c_{\text{CD}_3\text{OH}})_0 = (k_{\text{H}}/k_{\text{D}})_{\text{initial}} \quad (5)$$

k_{H} and k_{D} are the rate constants for the conversion of CH_3OH and CD_3OH , respectively. From Figure 6 we estimate $(k_{\text{H}}/k_{\text{D}})_{\text{initial}} = 3.0 \pm 0.3$. This value is significantly higher than all the slopes taken from the educt disappearance kinetics. It indicates that the initial reaction mechanism is different from that prevailing at later reaction stages. Note that both approaches, educt- and product-based, measure apparent intermolecular H-KIEs = $(k_{\text{H}}/k_{\text{D}})_{\text{intermolec.}}$.

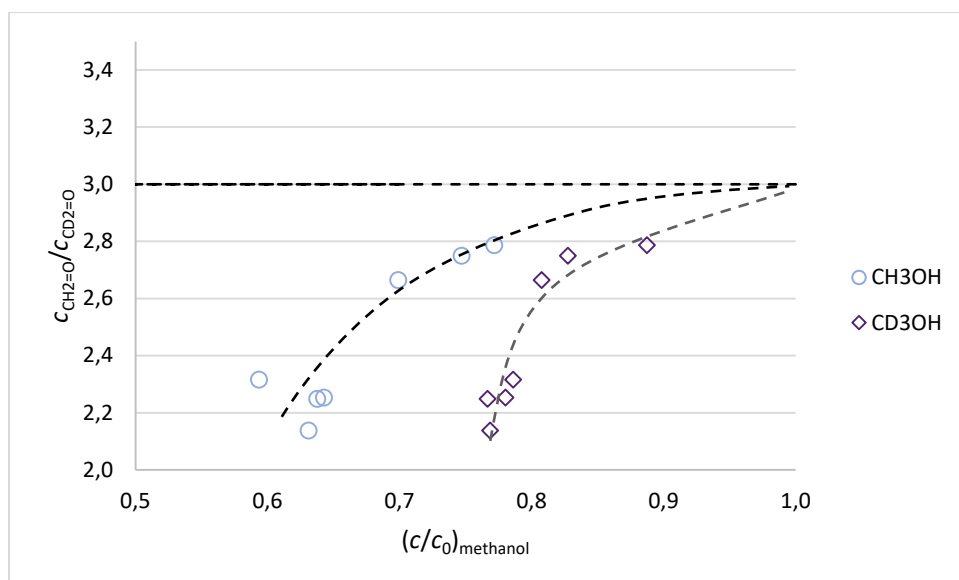


Figure 6: Oxidation of CH_3OH and CD_3OH (12 mM each) with PS (20 mM), activated by FeS (0.5 g L^{-1}) in suspension. Isotope composition of the formed formaldehyde ($c_{\text{CH}_2=\text{O}}/c_{\text{CD}_2=\text{O}}$) along the reaction progress. Extrapolation to zero methanol conversion ($c/c_0 \rightarrow 1.0$). The $c_{\text{CH}_2=\text{O}}/c_{\text{CD}_2=\text{O}}$ values are normalized to $(c_{\text{CH}_3\text{OH}}/c_{\text{CD}_3\text{OH}})_0 = 1$.

In order to verify the initial H-KIE and resolve the discrepancy of the previous values, the intramolecular H-KIE for formaldehyde formation from CHD₂OH was determined. In the case of intramolecular H-KIEs, the competition between H- and D-abstraction by the attacking radicals takes place in the same molecule. Unlike CH₃OH/CD₃OH mixtures, the isotopic composition of the substrate (CHD₂OH) remains constant during methanol conversion. Therefore, the slope of the isotopic composition of formaldehyde vs. methanol conversion is small and the accuracy of the extrapolated value is higher.

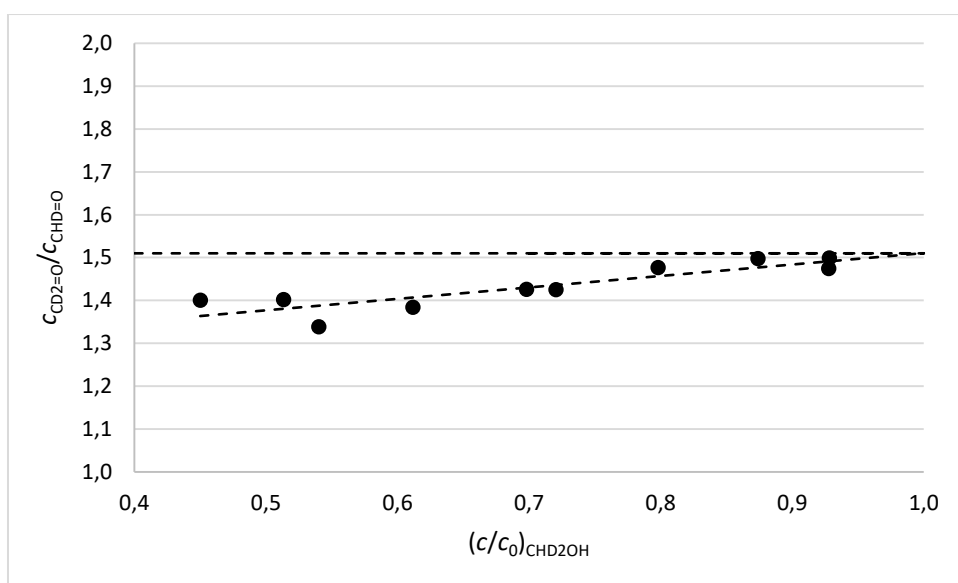


Figure 7: Oxidation of CHD₂OH (12 mM) with PS (10 mM), activated by FeS (0.5 g L⁻¹) in suspension. Isotope composition of the formed formaldehyde along the reaction progress. pH = 3.0-2.5.

Figure 7 shows the isotopic composition of formaldehyde formed from CHD₂OH. Thereby, a primary H-abstraction of methanol leads to CD₂=O, while a primary D-abstraction gives CHD=O. Due to the fact that in the parent molecule two D-abstractions and only one H-abstraction is possible, the statistical factor 2 for the intramolecular H-KIE per carbon-hydrogen bond must therefore be taken into account (eq. 6).

$$(k_{\text{H}}/k_{\text{D}})_{\text{intramolec}} = 2 \times (c_{\text{CD}_2=\text{O}} / c_{\text{CHD}=\text{O}})_{\text{X} \rightarrow 0} \quad (6)$$

Since formaldehyde is an intermediate and not a final product of methanol oxidation, its isotopic composition must again be extrapolated to a methanol conversion of zero. The intramolecular H-KIE thus obtained after accounting for the statistical factor is: $(k_H/k_D)_{\text{intramolec}} = 2 \times 1.51 = 3.02 \pm 0.05$. This value can be considered as the "true" or intrinsic KIE, as it is least affected by possible perturbations such as mass transfer limitation or previous adsorption steps. It agrees with the initial intermolecular H-KIE derived from the formaldehyde composition in the CH₃OH/CD₃OH competition experiment with FeS as activator. This means that H-KIE_{FeS} is 3.0, which is significantly higher than H-KIE_{hom} (2.3).

In summary: the measured H-KIEs for methanol oxidation in the presence of FeS do not clarify the reaction mechanism, but they give clear evidence of what it is not. The function of FeS is not (only) an assistance in the production of freely dissolved sulfate radicals from PS. Rather, FeS plays the role of a heterogeneous catalyst which assists in surface-associated substrate oxidation, as already postulated in section 3.1. This conclusion is based on the known H-KIE for hydrogen abstraction by freely dissolved sulfate radicals (Figure 4). One can hypothesize that the FeS-assisted oxidation involves surface-associated species which attack substrates such as methanol with a higher selectivity (higher H-KIE) than free sulfate radicals. Nevertheless, this does not preclude free sulfate radicals from contributing to the overall oxidation reaction, especially in the reaction system with methanol as a weakly adsorbing substrate.

4 Conclusions

In the framework of this study, the influence of the persulfate activator FeS on the selectivity of oxidation reactions was examined. Various chlorinated compounds from three classes were degraded with sulfate radicals generated by homogeneous or heterogeneous activation of persulfate. The obtained kinetic data show that freely dissolved sulfate radicals produced by thermal activation discriminates less between chlorine substitution patterns in a molecule, whereas the heterogeneous activation with FeS converts the same substance cocktail with a

higher selectivity. This leads to the hypothesis that sulfate radicals generated on the FeS surface react in the form of surface-associated radicals, which show a different selectivity than the freely dissolved sulfate radicals. This hypothesis was supported by measuring inter- and intramolecular hydrogen kinetic isotope effects for methanol oxidation, whereby the FeS-activated PS leads to a higher selectivity than the homogeneously activated PS. Therefore, it can be concluded that activation of PS using FeS as heterogeneous activator, and in most cases also the pollutant degradation itself, takes place mainly at the surface of the FeS rather than in solution. In addition, experiments using FeCA as a PS activator showed significantly different results in the selectivity pattern compared to thermal activation, which can be attributed to the formation of Fe^{4+} as a reactive species. Therefore, when using FeCA as an activator, caution should be used when interpreting rate constants and comparing activators.

ASSOCIATED CONTENT

Supporting Information. Supplementary data and methodical comments associated with this article can be found in the online version, at ...

Author Contributions

The manuscript was written with contributions of all authors. All authors have given approval to the final version of the manuscript.

The authors declare no competing financial interest.

ACKNOWLEDGEMENTS

This work was supported by funds of the German Federal Ministry of Education and Research (BMBF) in the frame of the project CONTASORB [grant number 03XP0090A].

References

1. Aikaterini Tsitonaki, Benjamin Petri, Michelle Crimi, Hans Mosbæk, Robert L. Siegrist, and Poul L. Bjerg, *In situ chemical oxidation of contaminated soil and groundwater using persulfate: A review*. *Critical Reviews in Environmental Science and Technology*, 2010. **40**(1): p. 55-91.
2. Fenglian Fu, Dionysios D. Dionysiou, and Hong Liu, *The use of zero-valent iron for groundwater remediation and wastewater treatment: A review*. *Journal of Hazardous Materials*, 2014. **267**: p. 194-205.
3. Marek Trojanowicz, Anna Bojanowska-Czajka, Iwona Bartosiewicz, and Krzysztof Kulisa, *Advanced oxidation/reduction processes treatment for aqueous perfluorooctanoate (pfoa) and perfluorooctanesulfonate (pfos) – a review of recent advances*. *Chemical Engineering Journal*, 2018. **336**: p. 170-199.
4. Raf Dewil, Dionissios Mantzavinos, Ioannis Poulios, and Manuel A. Rodrigo, *New perspectives for advanced oxidation processes*. *Journal of Environmental Management*, 2017. **195**: p. 93-99.
5. Ikechukwu A. Ike, Karl G. Linden, John D. Orbell, and Mikel Duke, *Critical review of the science and sustainability of persulphate advanced oxidation processes*. *Chemical Engineering Journal*, 2018. **338**: p. 651-669.
6. Stanisław Wacławek, Holger V. Lutze, Klaudiusz Grübel, Vinod V. T. Padil, Miroslav Černík, and Dionysios D. Dionysiou, *Chemistry of persulfates in water and wastewater treatment: A review*. *Chemical Engineering Journal*, 2017. **330**: p. 44-62.
7. David A. Armstrong, Robert E. Huie, Sergei Lymar, Willem H. Koppenol, Gabor Merényi, Pedatsur Neta, David M. Stanbury, Sten Steenken, and Peter Wardman, *Standard electrode potentials involving radicals in aqueous solution: Inorganic radicals*, in *BioInorganic Reaction Mechanisms*. 2013. p. 59-61.
8. P. Neta, V. Madhavan, Haya Zemel, and Richard W. Fessenden, *Rate constants and mechanism of reaction of sulfate radical anion with aromatic compounds*. *Journal of the American Chemical Society*, 1977. **99**(1): p. 163-164.
9. Shuang Luo, Zongsu Wei, Dionysios D. Dionysiou, Richard Spinney, Wei-Ping Hu, Liyuan Chai, Zhihui Yang, Tiantian Ye, and Ruiyang Xiao, *Mechanistic insight into reactivity of sulfate radical with aromatic contaminants through single-electron transfer pathway*. *Chemical Engineering Journal*, 2017. **327**: p. 1056-1065.
10. Stockholm Convention. *All pops listed in the stockholm convention*. 2019 28.02.2022]; Available from: <http://chm.pops.int/TheConvention/ThePOPs/AllPOPs/tabid/2509/Default.aspx>.
11. Robert E. Huie and Carol L. Clifton, *Rate constants for hydrogen abstraction reactions of the sulfate radical, so₄⁻. Alkanes and ethers*. *International Journal of Chemical Kinetics*, 1989. **21**(8): p. 611-619.
12. Carol L. Clifton and Robert E. Huie, *Rate constants for hydrogen abstraction reactions of the sulfate radical, so₄⁻. Alcohols*. *International Journal of Chemical Kinetics*, 1989. **21**(8): p. 677-687.
13. Kun-Chang Huang, Zhiqiang Zhao, George E. Hoag, Amine Dahmani, and Philip A. Block, *Degradation of volatile organic compounds with thermally activated persulfate oxidation*. *Chemosphere*, 2005. **61**(4): p. 551-560.
14. Guo-Dong Fang, Dionysios D. Dionysiou, Yu Wang, Souhail R. Al-Abed, and Dong-Mei Zhou, *Sulfate radical-based degradation of polychlorinated biphenyls: Effects of chloride ion and reaction kinetics*. *Journal of Hazardous Materials*, 2012. **227-228**: p. 394-401.
15. Ruiyang Xiao, Tiantian Ye, Zongsu Wei, Shuang Luo, Zhihui Yang, and Richard Spinney, *Quantitative structure–activity relationship (qsar) for the oxidation of trace organic contaminants by sulfate radical*. *Environmental Science & Technology*, 2015. **49**(22): p. 13394-13402.

16. Xin Zhu, Erdeng Du, Haoran Ding, Yusuo Lin, Tao Long, Huajie Li, and Lei Wang, *Qsar modeling of vocs degradation by ferrous-activated persulfate oxidation*. *Desalination and Water Treatment*, 2016. **57**(27): p. 12546-12560.
17. George V. Buxton, Clive L. Greenstock, W. Phillips Helman, and Alberta B. Ross, *Critical review of rate constants for reactions of hydrated electrons, hydrogen atoms and hydroxyl radicals (-oh/-o- in aqueous solution*. *Journal of Physical and Chemical Reference Data*, 1988. **17**(2): p. 513-886.
18. Laura W. Matzek and Kimberly E. Carter, *Activated persulfate for organic chemical degradation: A review*. *Chemosphere*, 2016. **151**(Supplement C): p. 178-188.
19. Ying-Hong Guan, Jun Ma, Yue-Ming Ren, Yu-Lei Liu, Jia-Yue Xiao, Ling-qiang Lin, and Chen Zhang, *Efficient degradation of atrazine by magnetic porous copper ferrite catalyzed peroxymonosulfate oxidation via the formation of hydroxyl and sulfate radicals*. *Water Research*, 2013. **47**(14): p. 5431-5438.
20. Tao Zhang, Haibo Zhu, and Jean-Philippe Croué, *Production of sulfate radical from peroxymonosulfate induced by a magnetically separable CuFe_2O_4 spinel in water: Efficiency, stability, and mechanism*. *Environmental Science & Technology*, 2013. **47**(6): p. 2784-2791.
21. Tao Zeng, Xiaole Zhang, Saihua Wang, Hongyun Niu, and Yaqi Cai, *Spatial confinement of a Co_3O_4 catalyst in hollow metal-organic frameworks as a nanoreactor for improved degradation of organic pollutants*. *Environmental Science & Technology*, 2015. **49**(4): p. 2350-2357.
22. Wen-Da Oh, Zhili Dong, and Teik-Thye Lim, *Generation of sulfate radical through heterogeneous catalysis for organic contaminants removal: Current development, challenges and prospects*. *Applied Catalysis B: Environmental*, 2016. **194**(Supplement C): p. 169-201.
23. Chenhui Zhao, Binbin Shao, Ming Yan, Zhifeng Liu, Qinghua Liang, Qingyun He, Ting Wu, Yang Liu, Yuan Pan, Jing Huang, Jiajia Wang, Jie Liang, and Lin Tang, *Activation of peroxymonosulfate by biochar-based catalysts and applications in the degradation of organic contaminants: A review*. *Chemical Engineering Journal*, 2021. **416**: p. 128829.
24. Songhu Yuan, Peng Liao, and Akram N. Alshawabkeh, *Electrolytic manipulation of persulfate reactivity by iron electrodes for trichloroethylene degradation in groundwater*. *Environmental Science & Technology*, 2014. **48**(1): p. 656-663.
25. Yueming Ren, Lingqiang Lin, Jun Ma, Jing Yang, Jing Feng, and Zhuangjun Fan, *Sulfate radicals induced from peroxymonosulfate by magnetic ferrosin MFe_2O_4 ($\text{M}=\text{Co}, \text{Cu}, \text{Mn}, \text{and Zn}$) as heterogeneous catalysts in the water*. *Applied Catalysis B: Environmental*, 2015. **165**(Supplement C): p. 572-578.
26. Ya-Ting Lin, Chenju Liang, and Chun-Wei Yu, *Trichloroethylene degradation by various forms of iron activated persulfate oxidation with or without the assistance of ascorbic acid*. *Industrial & Engineering Chemistry Research*, 2016. **55**(8): p. 2302-2308.
27. Yanlin Wu, Romain Prulho, Marcello Brigante, Wenbo Dong, Khalil Hanna, and Gilles Mailhot, *Activation of persulfate by Fe(III) species: Implications for 4-tert-butylphenol degradation*. *Journal of Hazardous Materials*, 2017. **322**: p. 380-386.
28. Rama Pulicharla, Roggy Drouinaud, Satinder Kaur Brar, Patrick Drogui, Francois Proulx, Mausam Verma, and Rao Y. Surampalli, *Activation of persulfate by homogeneous and heterogeneous iron catalyst to degrade chlortetracycline in aqueous solution*. *Chemosphere*, 2018. **207**: p. 543-551.
29. I. A. Ike and M. Duke, *Synthetic magnetite, maghemite, and haematite activation of persulphate for orange g degradation*. *Journal of Contaminant Hydrology*, 2018. **215**: p. 73-85.
30. P. Neta, Robert E. Huie, and Alberta B. Ross, *Rate constants for reactions of inorganic radicals in aqueous solution*. *Journal of Physical and Chemical Reference Data*, 1988. **17**(3): p. 1027-1284.

31. Seok-Young Oh, Seung-Gu Kang, Dong-Wook Kim, and Pei C. Chiu, *Degradation of 2,4-dinitrotoluene by persulfate activated with iron sulfides*. Chemical Engineering Journal, 2011. **172**(2): p. 641-646.
32. Yanmei Yuan, Hong Tao, Jinhong Fan, and Luming Ma, *Degradation of p-chloroaniline by persulfate activated with ferrous sulfide ore particles*. Chemical Engineering Journal, 2015. **268**(Supplement C): p. 38-46.
33. Hai Chen, Zhonglei Zhang, Mingbao Feng, Wei Liu, Wenjing Wang, Qi Yang, and Yuanan Hu, *Degradation of 2,4-dichlorophenoxyacetic acid in water by persulfate activated with fes (mackinawite)*. Chemical Engineering Journal, 2017. **313**: p. 498-507.
34. Jinhong Fan, Lin Gu, Deli Wu, and Zhigang Liu, *Mackinawite (fes) activation of persulfate for the degradation of p-chloroaniline: Surface reaction mechanism and sulfur-mediated cycling of iron species*. Chemical Engineering Journal, 2018. **333**: p. 657-664.
35. Sarah Sühnhholz, Frank-Dieter Kopinke, and Katrin Mackenzie, *Reagent or catalyst? – fes as activator for persulfate in water*. Chemical Engineering Journal, 2020. **387**: p. 123804.
36. Sarah Sühnhholz, Alina Gawel, Frank-Dieter Kopinke, and Katrin Mackenzie, *Evidence of heterogeneous degradation of pfoa by activated persulfate – fes as adsorber and activator*. Chemical Engineering Journal, 2021. **423**: p. 130102.
37. Zhen Wang, Wei Qiu, Su-yan Pang, Yang Zhou, Yuan Gao, Chaoting Guan, and Jin Jiang, *Further understanding the involvement of fe(iv) in peroxydisulfate and peroxymonosulfate activation by fe(ii) for oxidative water treatment*. Chemical Engineering Journal, 2019. **371**: p. 842-847.
38. Hongyu Dong, Yang Li, Shuchang Wang, Weifan Liu, Gongming Zhou, Yifan Xie, and Xiaohong Guan, *Both fe(iv) and radicals are active oxidants in the fe(ii)/peroxydisulfate process*. Environmental Science & Technology Letters, 2020. **7**(3): p. 219-224.
39. Virender K. Sharma, *Oxidation of inorganic contaminants by ferrates (vi, v, and iv)–kinetics and mechanisms: A review*. Journal of Environmental Management, 2011. **92**(4): p. 1051-1073.
40. Jiahui Zhu, Fulu Yu, Jiaoran Meng, Binbin Shao, Hongyu Dong, Wenhai Chu, Tongcheng Cao, Guangfeng Wei, Hejia Wang, and Xiaohong Guan, *Overlooked role of fe(iv) and fe(v) in organic contaminant oxidation by fe(vi)*. Environmental Science & Technology, 2020. **54**(15): p. 9702-9710.
41. Hengduo Xu and Yanqing Sheng, *New insights into the degradation of chloramphenicol and fluoroquinolone antibiotics by peroxymonosulfate activated with fes: Performance and mechanism*. Chemical Engineering Journal, 2021. **414**: p. 128823.
42. Frank-Dieter Kopinke and Anett Georgi, *What controls selectivity of hydroxyl radicals in aqueous solution? Indications for a cage effect*. The Journal of Physical Chemistry A, 2017. **121**(41): p. 7947-7955.
43. Y.-R. Luo, *Comprehensive handbook of chemical bond energies (1st ed.)*. 2007: CRC Press.
44. Kousik Kundu, Sarah F. Knight, Seungjun Lee, W. Robert Taylor, and Niren Murthy, *A significant improvement of the efficacy of radical oxidant probes by the kinetic isotope effect*. Angewandte Chemie International Edition, 2010. **49**(35): p. 6134-6138.
45. Bingzhi Li, Lin Li, Kuangfei Lin, Wei Zhang, Shuguang Lu, and Qishi Luo, *Removal of 1,1,1-trichloroethane from aqueous solution by a sono-activated persulfate process*. Ultrasonics Sonochemistry, 2013. **20**(3): p. 855-863.
46. R. J. Xie, J. P. Cao, X. W. Xie, D. X. Lei, K. H. Guo, H. Liu, Y. X. Zeng, and H. B. Huang, *Mechanistic insights into complete oxidation of chlorobenzene to co2 via wet scrubber coupled with uv/pds*. Chemical Engineering Journal, 2020. **401**: p. 13.
47. Zhen Wang, Wei Qiu, Suyan Pang, Yuan Gao, Yang Zhou, Ying Cao, and Jin Jiang, *Relative contribution of ferryl ion species (fe(iv)) and sulfate radical formed in nanoscale zero valent iron activated peroxydisulfate and peroxymonosulfate processes*. Water Research, 2020. **172**: p. 115504.

48. Changyin Zhu, Fengxiao Zhu, Cun Liu, Ning Chen, Dongmei Zhou, Guodong Fang, and Juan Gao, *Reductive hexachloroethane degradation by $S_2O_8^{\bullet-}$ with thermal activation of persulfate under anaerobic conditions*. *Environmental Science & Technology*, 2018. **52**(15): p. 8548-8557.
49. G. Merga, C. T. Aravindakumar, B. S. M. Rao, H. Mohan, and J. P. Mittal, *Pulse-radiolysis study of the reactions of $SO_4^{\bullet-}$ radical-ion with some substituted benzenes in aqueous-solution*. *Journal of the Chemical Society-Faraday Transactions*, 1994. **90**(4): p. 597-604.
50. Martin Elsner, Luc Zwank, Daniel Hunkeler, and René P. Schwarzenbach, *A new concept linking observable stable isotope fractionation to transformation pathways of organic pollutants*. *Environmental Science & Technology*, 2005. **39**(18): p. 6896-6916.

Supplementary material

Heterogeneous activation of persulfate by FeS – Surface influence on selectivity.

Sarah Sühnholz^{*a,b}, *Frank-Dieter Kopinke*^a and *Katrin Mackenzie*^a

^aHelmholtz Centre for Environmental Research - UFZ, Department of Environmental Engineering, Permoserstr. 15, D-04318 Leipzig, Germany

^bIntrapore GmbH, Katernberger Str. 107, D-45327 Essen, Germany

Corresponding Author

*Email: sarah.suehnholz@ufz.de. Phone: +49 3412351698.

Content

1	Kinetic considerations for system comparison	2
2	Selectivity of sulfate radicals generated by various PS activation methods	3
2.1	Chlorinated ethenes	3
2.2	Chlorinated ethanes	5
2.3	Chlorinated benzenes	7
3	Apparent second-order rate constants	9
4	Estimation of Fe(IV) participation	11

1 Kinetic considerations for system comparison

The double-logarithmic plot of relative concentrations of two substances is based on the following rate equations on the reaction kinetics:

$$-\frac{dc_1}{dt} = \sum (k_{1,R_i} \cdot c_1 \cdot c_{R_i}) \quad (\text{SI1})$$

with c_1 and c_{R_i} as the concentrations of the target compound 1 (e.g. PCE or CH₃OH or CD₃OH) and the reactive radicals R_i, e.g. sulfate radicals or chlorine atoms etc. k_{1,R_i} is the second-order rate constant of the H(D)-abstraction or electron transfer by the radical R_i from the target component 1. The sum is formed over all reactive radicals R_i in the solution.

When considering the conversion of a binary mixture of the components 1 and 2, it results eq. SI2.

$$\frac{dc_1}{dc_2} = \frac{\sum (k_{1,R_i} \cdot c_1 \cdot c_{R_i})}{\sum (k_{2,R_i} \cdot c_2 \cdot c_{R_i})} \quad (\text{SI2})$$

$$\frac{\ln \frac{c_1}{c_{1,0}}}{\ln \frac{c_2}{c_{2,0}}} = \frac{\sum (k_{1,R_i} \cdot c_{R_i})}{\sum (k_{2,R_i} \cdot c_{R_i})} \quad (\text{SI3})$$

with $c_{1,0}$ and $c_{2,0}$ as the initial concentrations of the two components 1 and 2. When plotting $\ln(c_1/c_{1,0})$ vs. $\ln(c_2/c_{2,0})$, $[\sum (k_{1,R_i} \cdot c_{R_i})] / [\sum (k_{2,R_i} \cdot c_{R_i})]$ is the slope at any point of the regression curve along the substrate conversion. In case of dominance of only one reactive radical R_i or a constant (stationary) pool of reactive radicals the slope is constant over the entire conversion range. It results a linear regression line. The slope of this line is the ratio $k_{1,R_i}/k_{2,R_i} = (k_1/k_2)_{R_i}$. In case of components 1 and 2 are isotopologues of a compound, this ratio is equivalent to a kinetic isotope effect (KIE) $(k_H/k_D)_{R_i}$.

When the pool of reactive radicals is changing along the substrate conversion ($c_1/c_{1,0}$), the value of the quotient on the right side of eqs. SI2 and 3 may vary, depending on the selectivities of the radicals $(k_1/k_2)_{R_i}$ and their concentration ratios (c_{R_i}/c_{R_j}) . In case of a significant conversion of

sulfate radicals into chlorine radicals (in the presence of chloride) or OH radicals (in the presence of OH⁻) this would (most likely) result in a curved regression line in the double-logarithmic concentration plot. Such a curvature was not observed in most competition experiments.

2 Selectivity of sulfate radicals generated by various PS activation methods

2.1 Chlorinated ethenes

2.1.1 PS activation with FeS

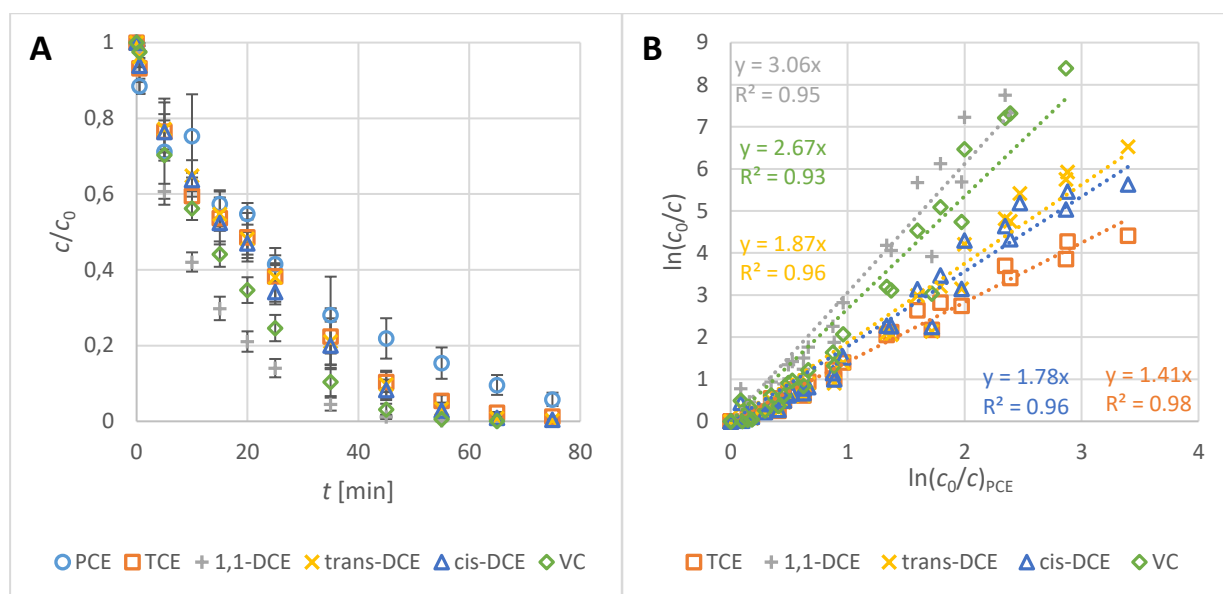


Figure S11: A) Degradation of chlorinated ethenes with sulfate radicals and B) competition kinetics of chlorinated ethenes oxidation with sulfate radicals related to PCE oxidation. Sulfate radicals were generated by activation of PS with FeS ($c_{0,\text{each chloroethene}} = 120 \mu\text{M}$; $c_{0,\text{FeS}} = 0.3 \text{ g L}^{-1}$; $c_{0,\text{PS}} = 4 \text{ mM}$; $\text{pH}_{\text{start}} = 7$; $\text{pH}_{\text{final}} = 2.4$). The error bars are the average deviation of single values from the mean value from three replicate experiments.

2.1.2 PS activation with FeCA

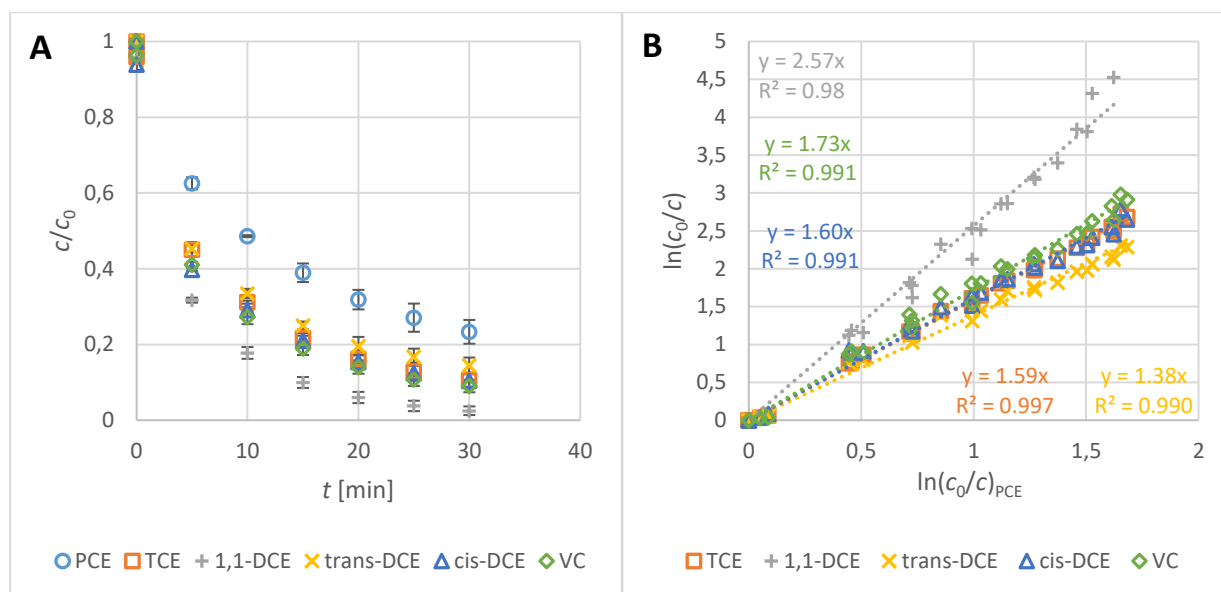


Figure SI2: A) Degradation of chlorinated ethenes with sulfate radicals and B) competition kinetics of chlorinated ethenes oxidation with sulfate radicals related to PCE oxidation. Sulfate radicals were generated by activation of PS with FeCA ($c_{0,\text{each chloroethene}} = 120 \mu\text{M}$; $c_{0,\text{FeCA}} = 5.4 \text{ mM}$; $c_{0,\text{PS}} = 4 \text{ mM}$; $\text{pH}_{\text{start}} = 7$; $\text{pH}_{\text{final}} = 2.4$). The error bars are average deviations of single values from the mean value from three replicate experiments.

2.1.3 Thermal PS activation

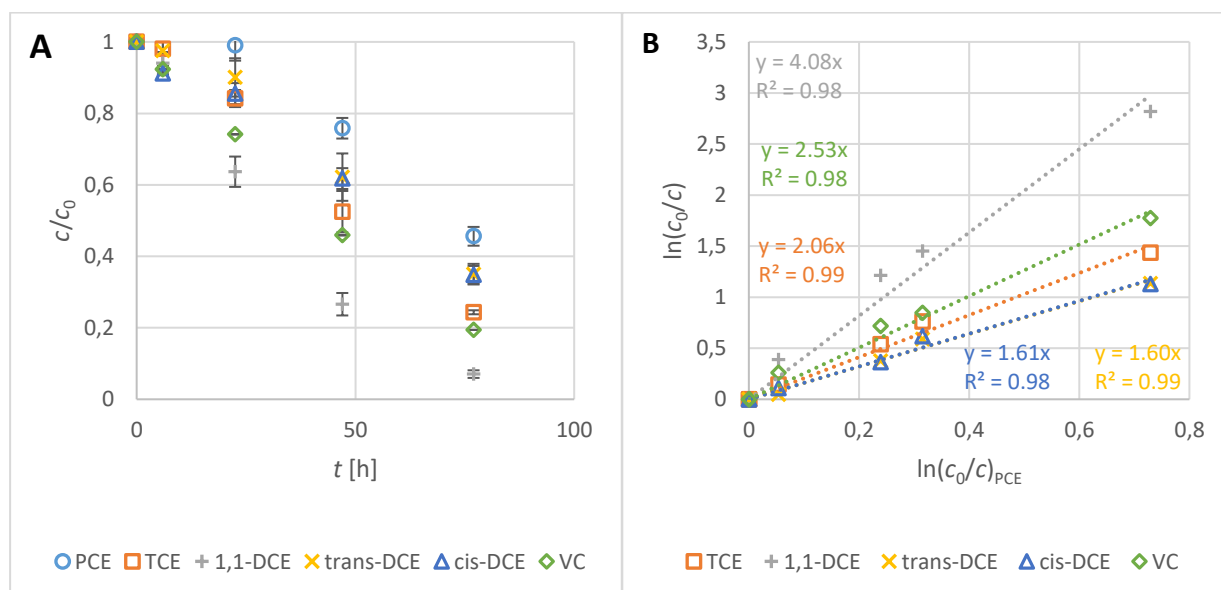


Figure SI3: A) Degradation of chlorinated ethenes with sulfate radicals and B) competition kinetics of chlorinated ethenes oxidation with sulfate radicals related to PCE oxidation. Sulfate radicals were generated by thermal activation of PS at $T = 30^\circ\text{C}$ ($c_{0,\text{each chloroethene}} = 120 \mu\text{M}$; $c_{0,\text{PS}} = 4 \text{ mM}$; $\text{pH}_{\text{start}} = 7$; $\text{pH}_{\text{final}} = 2.5$). The indicated error bars are average deviations from the mean value from two replicate experiments.

2.2 Chlorinated ethanes

2.2.1 PS activation with FeS

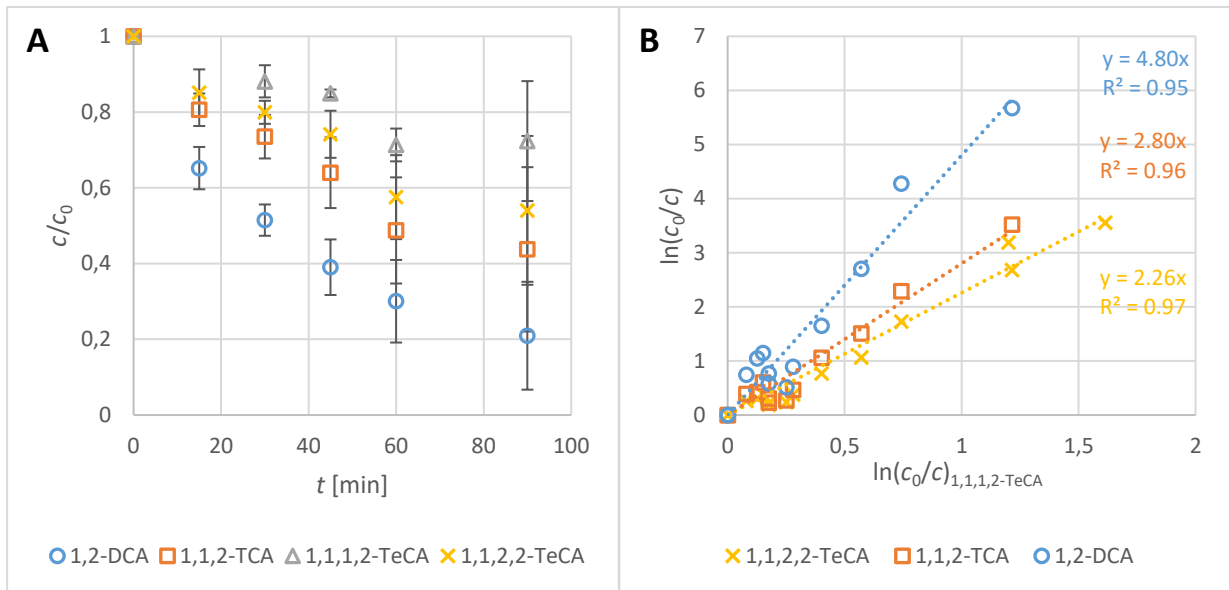


Figure SI4: A) Degradation of chlorinated ethanes with sulfate radicals and B) competition kinetics of chlorinated ethanes oxidation with sulfate radicals related to 1,1,1,2-TeCA oxidation. Sulfate radicals were generated by activation of PS with FeS ($c_{0,\text{each chloroethane}} = 30 \mu\text{M}$; $c_{0,\text{FeS}} = 0.3 \text{ g L}^{-1}$; $c_{0,\text{PS}} = 4 \text{ mM}$; $\text{pH}_{\text{start}} = 7$; $\text{pH}_{\text{final}} = 2.4$). The indicated error bars are average deviations from the mean value from three replicate experiments.

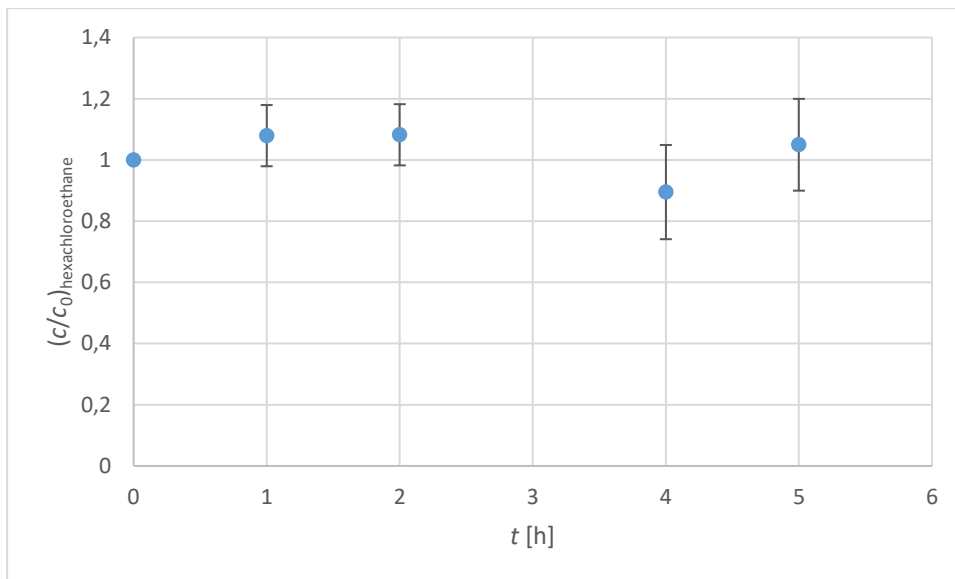


Figure SI5: Degradation of hexachloroethane with sulfate radicals. Sulfate radicals were generated by activation of PS with FeS ($c_{0,\text{hexachloroethane}} = 30 \mu\text{M}$; $c_{0,\text{FeS}} = 0.3 \text{ g L}^{-1}$; $c_{0,\text{PS}} = 4 \text{ mM}$; $\text{pH}_{\text{start}} = 7$; $\text{pH}_{\text{final}} = 2.4$). The indicated error bars are average deviations from the mean value from two replicate experiments.

2.2.2 Thermal PS activation

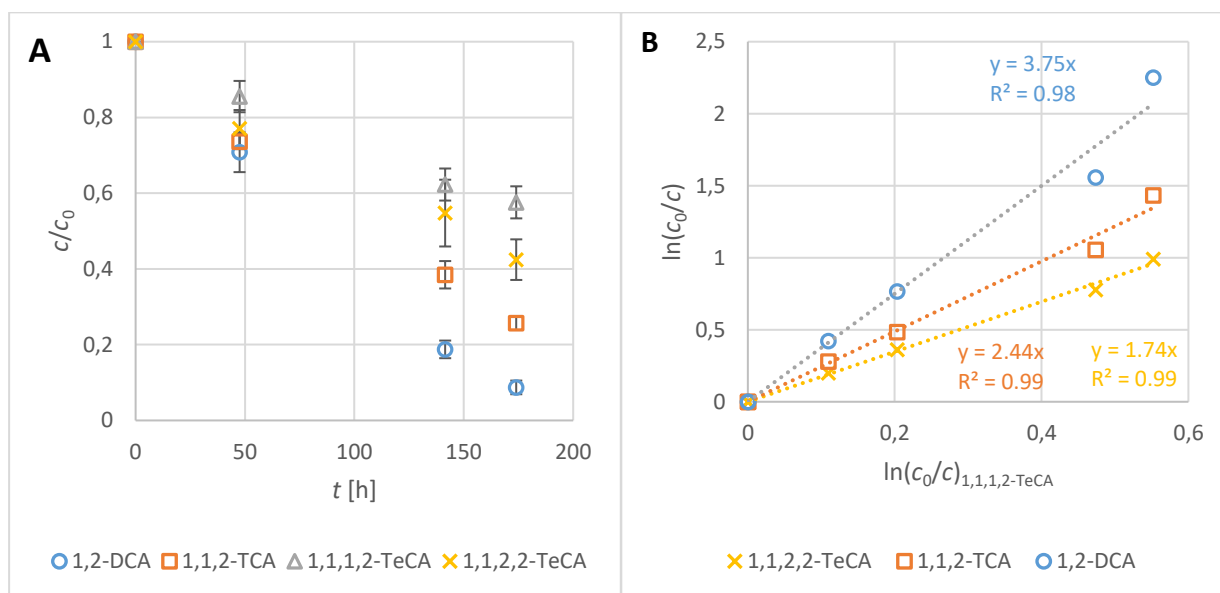


Figure SI6: A) Degradation of chlorinated ethanes with sulfate radicals and B) competition kinetics of chlorinated ethanes oxidation with sulfate radicals related to 1,1,1,2-TeCA oxidation. Sulfate radicals were generated by thermal activation of PS with $T = 30^\circ\text{C}$ ($c_{0,\text{each chloroethane}} = 30 \mu\text{M}$; $c_{0,\text{PS}} = 4 \text{ mM}$; $\text{pH}_{\text{start}} = 7$; $\text{pH}_{\text{final}} = 2.6$). The indicated error bars are the deviation from the mean value from two replicate experiments.

Figure SI6A reveals that the degradation of chloroethanes does apparently not follow first-order kinetics. However, $c_i = f(t)$ as shown in Figure SI6A does not necessarily reflect the reaction order with respect to c_i , rather it reflects the complex overall kinetics inclusive radical concentrations along the reaction time. The applicability of the used data evaluation method (eq. 3 in the main part) is validated by the linearity of correlation lines in the double-logarithmic plot (Figure SI6B).

2.3 Chlorinated benzenes

2.3.1 PS activation with FeS

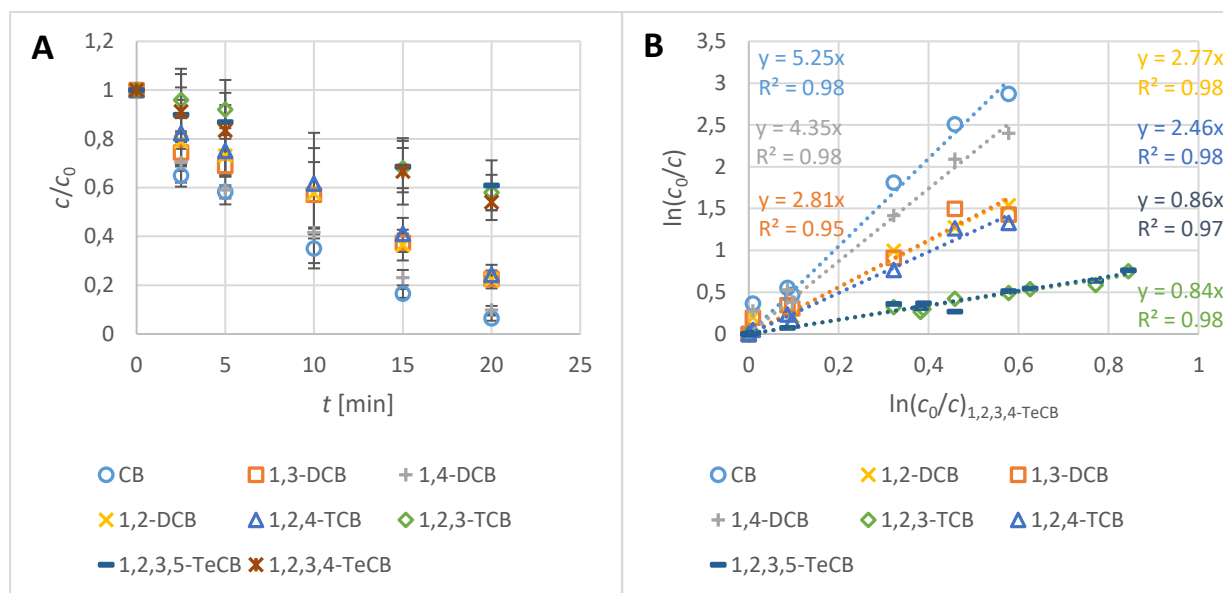


Figure SI7: A) Degradation of chlorinated benzenes with sulfate radicals and B) competition kinetics of chlorinated benzene oxidation with sulfate radicals related to 1,2,3,4-TeCB oxidation. Sulfate radicals were generated by activation of PS with FeS (c_0 , each chlorobenzene = 20 μM ; c_0 , FeS = 0.3 g L^{-1} ; c_0 , PS = 4 mM; $\text{pH}_{\text{start}} = 7$; $\text{pH}_{\text{final}} = 2.4$). The indicated error bars are the deviation from the mean value from three replicate experiments.

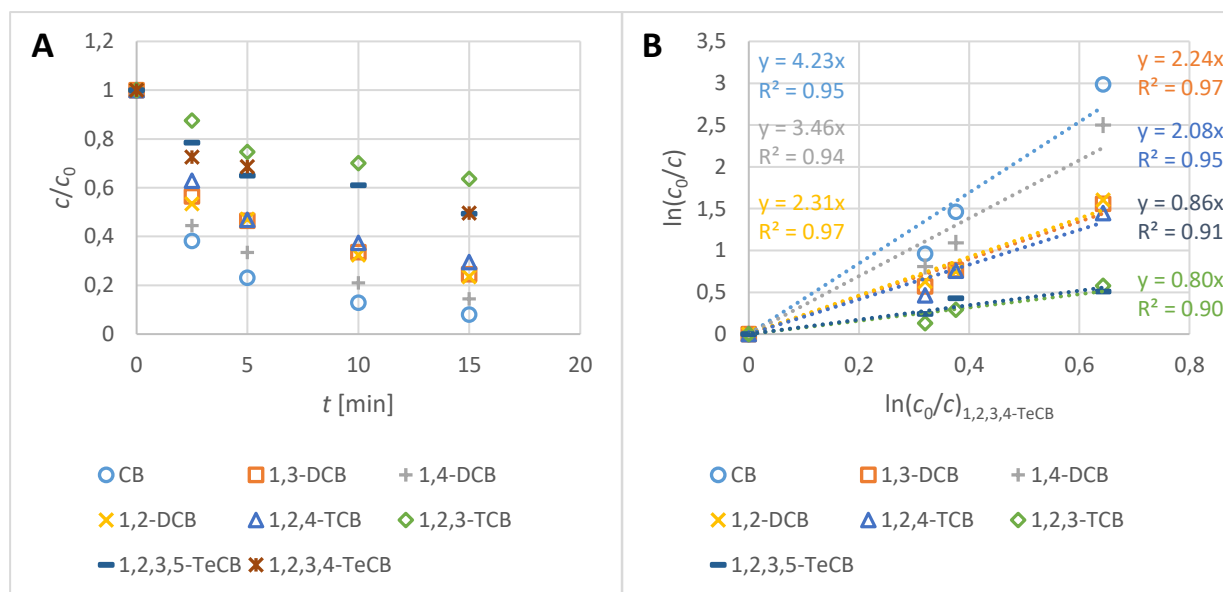


Figure SI8: A) Degradation of chlorinated benzenes with sulfate radicals and B) competition kinetics of chlorinated benzene oxidation with sulfate radicals related to 1,2,3,4-TeCB oxidation. Sulfate radicals were generated by activation of PS with FeS (c_0 , each chlorobenzene = 20 μM ; c_0 , FeS = 0.3 g L^{-1} ; c_0 , PS = 4 mM; $\text{pH}_{\text{start}} = 3$).

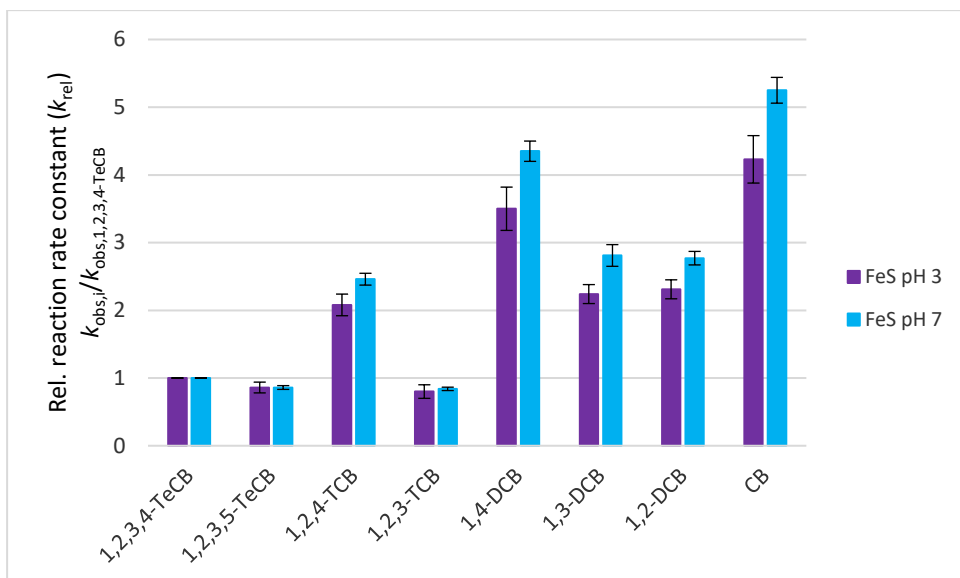


Figure SI9: Relative reaction rate constants of chlorinated benzene reaction with sulfate radicals. Sulfate radicals were generated by activation of PS with FeS at different starting pH ($c_{0,\text{each chlorobenzene}} = 20 \mu\text{M}$; $c_{0,\text{FeS}} = 0.3 \text{ g L}^{-1}$; $c_{0,\text{PS}} = 4 \text{ mM}$; $\text{pH}_{\text{start}} = 3$ or 7). The error bars represent standard deviations of slopes of regression lines.

2.3.2 PS activation with FeCA

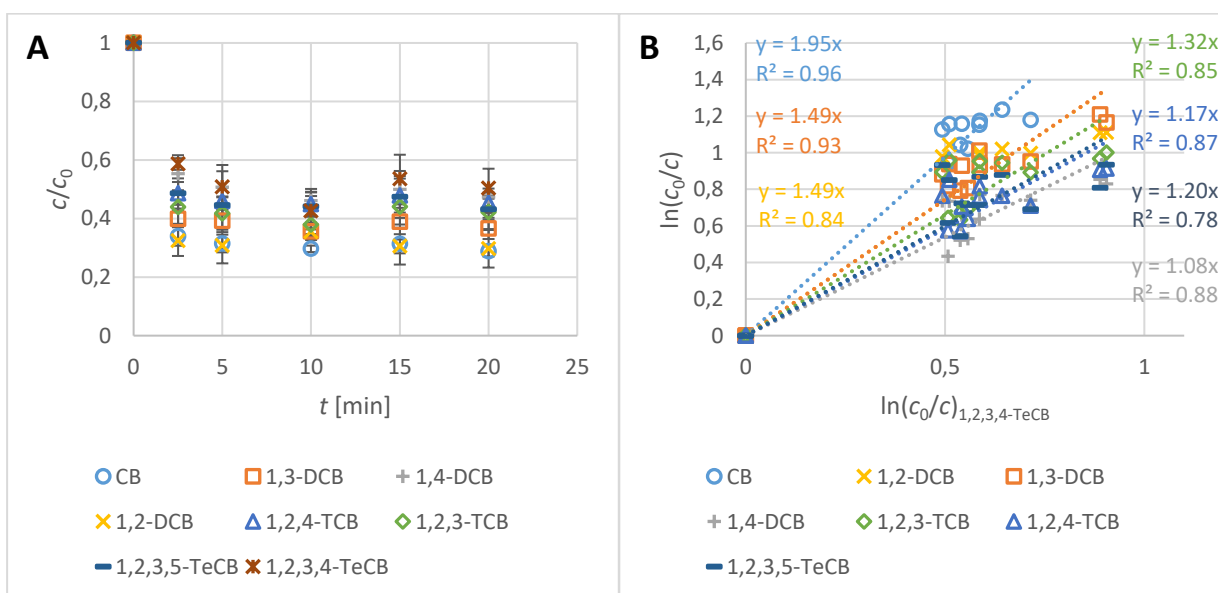


Figure SI10: A) Degradation of chlorinated benzenes with sulfate radicals and B) competition kinetics of chlorinated benzene oxidation with sulfate radicals related to 1,2,3,4-TeCB oxidation. Sulfate radicals were generated by activation of PS with FeCA ($c_{0,\text{each chlorobenzene}} = 20 \mu\text{M}$; $c_{0,\text{FeCA}} = 5.4 \text{ mM}$; $c_{0,\text{PS}} = 4 \text{ mM}$; $\text{pH}_{\text{start}} = 7$; $\text{pH}_{\text{final}} = 2.4$). The indicated error bars are the deviation from the mean value from three replicate experiments.

2.3.3 Thermal PS activation

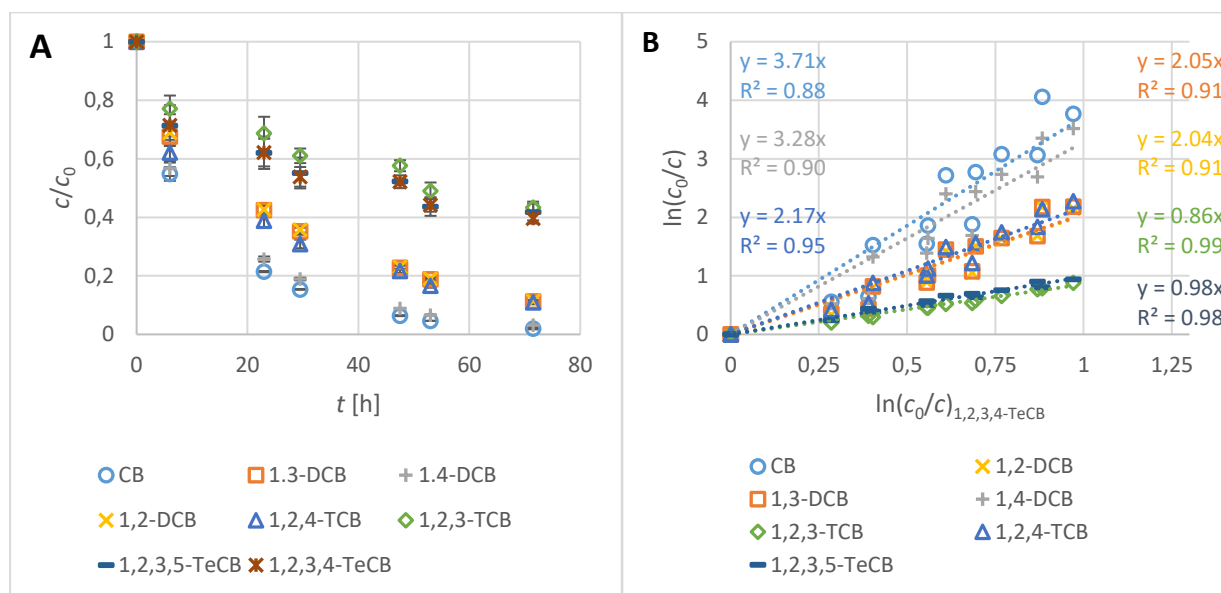


Figure SI11: A) Degradation of chlorinated benzenes with sulfate radicals and B) competition kinetics of chlorinated benzene oxidation with sulfate radicals related to 1,2,3,4-TeCB oxidation. Sulfate radicals were generated by thermal activation of PS at $T = 30^\circ\text{C}$ ($c_{0,\text{each chlorobenzene}} = 20 \mu\text{M}$; $c_{0,\text{PS}} = 4 \text{mM}$; $\text{pH}_{\text{start}} = 7$; $\text{pH}_{\text{final}} = 3.4$). The indicated error bars are the deviation from the mean value from three replicate experiments.

Figure SI11A shows that the degradation is only just beginning. Due to the low degree of conversion, the measured concentrations are less than 25 % different from $c_{0,\text{chlorinated substance}}$, thus the results are prone to higher uncertainty. However, since the values are reproducible, we decided to consider the experiment and show the results here.

3 Apparent second-order rate constants

Experimental: The reactions were carried out in 60 mL crimped serum bottles with starting concentrations of PCE, 1,2-DCA and CB of 0.02 mM in 50 mL aqueous solution in two separate cocktails. In the competition kinetics experiment with 1,2-DCA and CB and PCE and CB, heat activation of PS at 30°C was used. The gas phase was sampled and analyzed using a GC-MS device for competition kinetics with PCE and CB. 1 mL aqueous samples were taken and extracted with chloroform for competition kinetics of 1,2-DCA and CB (spiked with toluene- d_8 as internal standard). The addition of 1 mL of PS stock solution (200 mM) to the bottles marked the reaction start (t_0). Periodically, the gas phase was analyzed with GC-MS directly (PCE and CB) or 1 mL aqueous samples (maximum 10% of the total volume) were collected from the

bottles for extraction (1,2-DCA and CB), whereby the extracts were analyzed by means of GC-MS-QP2010.

Results: The apparent second-order rate constants of PCE and 1,2-DCA with $\text{SO}_4^{\cdot-}$ were determined on the basis of competition kinetics. CB was selected as a reference compound with known second-order rate constant of $k_{\text{CB}}^{\text{SO}_4^{\cdot-}}, 20^\circ\text{C} = 1.5 \times 10^9 \text{ M}^{-1}\text{s}^{-1}$ at 20°C [1]. This value can also be used for homogeneous activation at 30°C . The reason for this is that the differences between the activation energies of the individual compounds are (presumably) small and the difference between 20°C and 30°C is only a few Kelvin. Together, this results in only small uncertainties in the reaction rate constant ($<10\%$). For two solutes A and B undergoing rate-limiting elementary bimolecular reactions with a common reactant, e.g. $\text{SO}_4^{\cdot-}$ (eq. SI4), in the same homogeneous reaction solution, the rate laws are as shown in eqs. SI5 and SI6:



$$\frac{dc_{\text{A}}}{dt} = -k_{\text{A}}^{\text{SO}_4^{\cdot-}} \cdot c_{\text{SO}_4^{\cdot-}} \cdot c_{\text{A}} \quad (\text{SI5})$$

$$\frac{dc_{\text{B}}}{dt} = -k_{\text{B}}^{\text{SO}_4^{\cdot-}} \cdot c_{\text{SO}_4^{\cdot-}} \cdot c_{\text{B}} \quad (\text{SI6})$$

$$\frac{dc_{\text{A}}}{dc_{\text{B}}} = \frac{k_{\text{A}}^{\text{SO}_4^{\cdot-}} c_{\text{A}}}{k_{\text{B}}^{\text{SO}_4^{\cdot-}} c_{\text{B}}} \quad (\text{SI7})$$

Since the concentration of $\text{SO}_4^{\cdot-}$ is identical in eqs. SI5 and SI6 at any time t , they can be combined to eq. SI7. By integration, eq. SI8 is obtained, which shows that the ratio of the rate constants for reactions with sulfate radicals for the two compounds A and B can be determined from a double-logarithmic plot of the residual relative concentrations of the two compounds (see Figure S12).

$$\ln \frac{c_{\text{A},t}}{c_{\text{A},0}} = \frac{k_{\text{A}}^{\text{SO}_4^{\cdot-}}}{k_{\text{B}}^{\text{SO}_4^{\cdot-}}} \ln \frac{c_{\text{B},t}}{c_{\text{B},0}} \quad (\text{SI8})$$

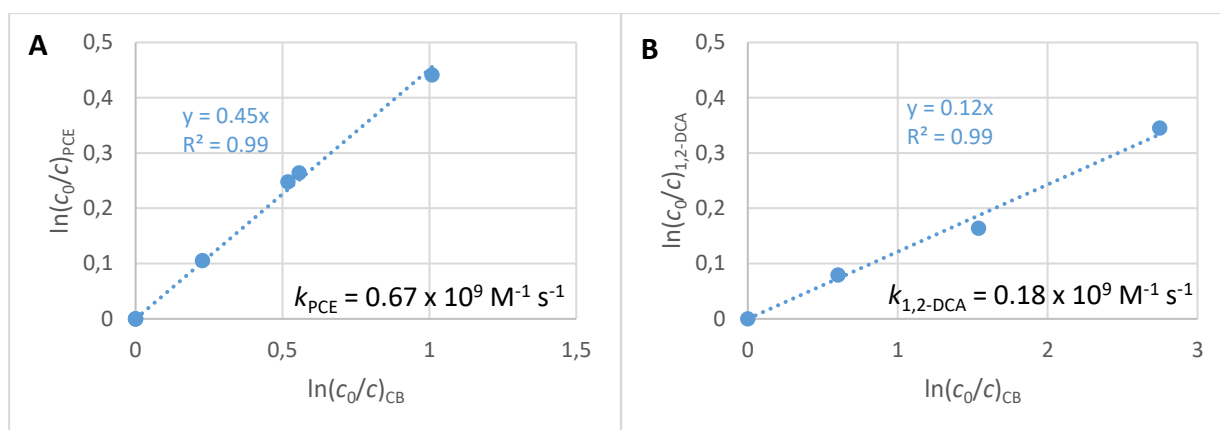


Figure SII2: A) Competition kinetic plots and the calculated apparent second-order rate constants for the reaction of PCE with SO_4^- ($c_{0,\text{PCE}} = c_{0,\text{CB}} = 20 \mu\text{M}$; $T = 30^\circ\text{C}$; $c_{0,\text{PS}} = 4 \text{ mM}$; $\text{pH}_{\text{start}} = 7$; $\text{pH}_{\text{final}} = 2.4$). B) Competition kinetic plots and the calculated apparent second-order rate constants for the reaction of 1,2-DCA with SO_4^- ($c_{0,1,2\text{-DCA}} = c_{0,\text{CB}} = 20 \mu\text{M}$; $T = 30^\circ\text{C}$; $c_{0,\text{PS}} = 4 \text{ mM}$; $\text{pH}_{\text{start}} = 7$; $\text{pH}_{\text{final}} = 2.4$).

4 Estimation of Fe(IV) participation

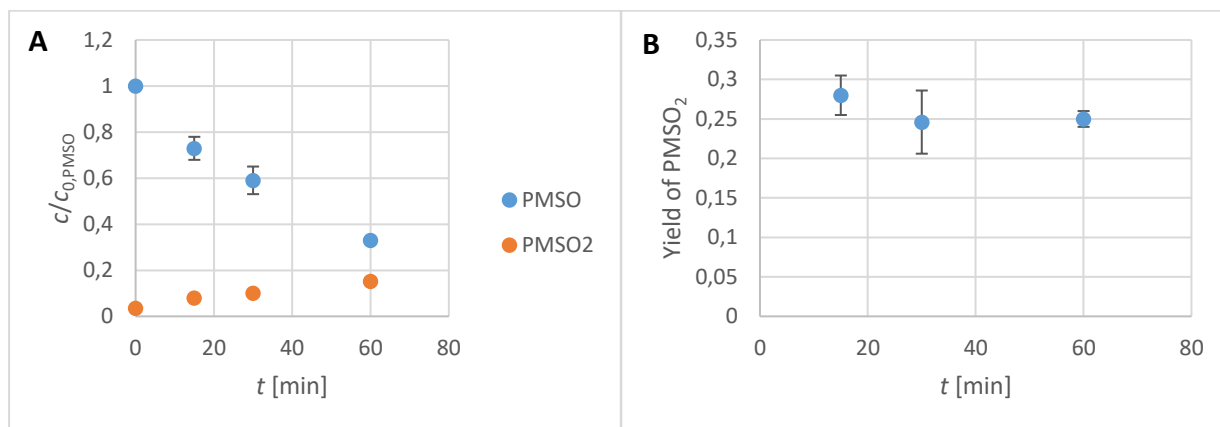


Figure SII3: A) Degradation of methyl phenyl sulfoxide (PMSO) with FeCA activated PS and formation of methyl phenyl sulfone (PMSO₂) B) Yield of PMSO₂ over time. ($c_{0,\text{PMSO}} = 10 \text{ mg L}^{-1}$; $c_{0,\text{FeCA}} = 5.4 \text{ mM}$; $c_{0,\text{PS}} = 4 \text{ mM}$; $\text{pH}_{\text{start}} = 7$; $\text{pH}_{\text{final}} = 2.4$). The indicated error bars are the deviation from the mean value from two replicate experiments.

In order to evaluate the contribution of Fe^{4+} in the activation of PS with FeCA, methyl phenyl sulfoxide (PMSO) was used as a probe compound. It is known that PMSO is oxidized by Fe^{4+} species to the corresponding sulfone (methyl phenyl sulfone (PMSO₂)), while sulfate radicals oxidize PMSO to biphenyl compounds [3]. Therefore, the yield of PMSO₂ provides information about the involvement of the reactive species. As can be seen in Figure SII3, the yield of PMSO₂ is about 25% and, therefore, the oxidant Fe^{4+} could markedly influence the selectivity pattern.

References

1. G. Merga, C.T. Aravindakumar, B.S.M. Rao, H. Mohan, and J.P. Mittal, *Pulse-radiolysis study of the reactions of SO_4^- -radical-ion with some substituted benzenes in aqueous-solution*. Journal of the Chemical Society-Faraday Transactions, 1994. **90**(4): p. 597.

2. C.M. Dominguez, A. Romero, D. Lorenzo, and A. Santos, *Thermally activated persulfate for the chemical oxidation of chlorinated organic compounds in groundwater*. Journal of Environmental Management, 2020. **261**: p. 110240.
3. Zhen Wang, Wei Qiu, Su-yan Pang, Yang Zhou, Yuan Gao, Chaoting Guan, and Jin Jiang, *Further understanding the involvement of Fe(IV) in peroxydisulfate and peroxymonosulfate activation by Fe(II) for oxidative water treatment*. Chemical Engineering Journal, 2019. **371**: p. 842-847.